Cell Reports
Medicine

Article

Regulation of LEAP2 by insulin and glucagon in mice and humans

Graphical abstract

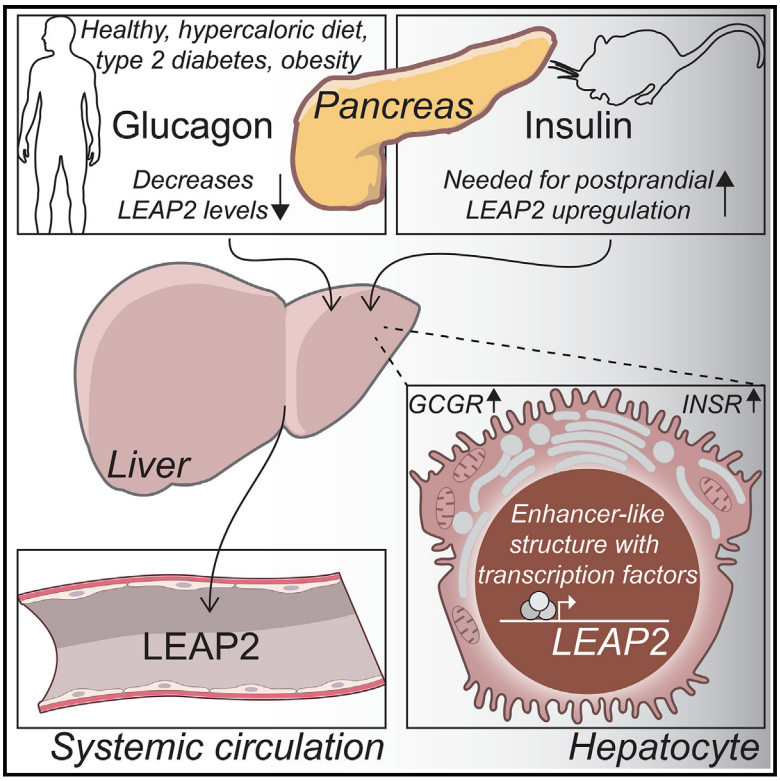

Highlights

- Plasma LEAP2 decreases upon glucagon infusions in humans
- This is preserved in patients with obesity and T2DM but diminished by a hypercaloric diet
- Postprandial LEAP2 upregulation is offset by insulin receptor antagonism in mice
- *INSR*- and *GCGR*-expressing hepatocytes are the main sources of hepatic *LEAP2* expression

Authors

Valdemar Brimnes Ingemann Johansen, Anna Katrina Jógvansdóttir Gradel, Stephanie Kjærulff Holm, ..., Kei Sakamoto, Birgitte Holst, Christoffer Clemmensen

Correspondence

chc@sund.ku.dk

In brief

Johansen and Gradel et al. investigate the endocrine regulation of LEAP2, an endogenous antagonist of the ghrelin receptor, in mice and humans. Their findings provide evidence that insulin and glucagon are key regulators of LEAP2 and warrant further investigations into the exact mechanisms orchestrating this endocrine axis.

Johansen et al., 2025, Cell Reports Medicine *6*, 101996
March 18, 2025
https://doi.org/10.1016/j.xcrm.2025.101996

CellPress

Cell Reports Medicine

CellPress
OPEN ACCESS

Article

Regulation of LEAP2 by insulin and glucagon in mice and humans

Valdemar Brimnes Ingemann Johansen,[1,2,3,15] Anna Katrina Jógvansdóttir Gradel,[2,10,11,12,15] Stephanie Kjærulff Holm,[1] Joyceline Cuenco,[1] Christoffer Merrild,[1] Natalia Petersen,[3] Damien Demozay,[3] Bharath Kumar Mani,[4] Malte Palm Suppli,[5] Magnus F.G. Grøndahl,[5] Asger Bach Lund,[5,6,7] Filip Krag Knop,[5,6,7,13] Cesar A. Prada-Medina,[8] Wouter Frederik Johan Hogendorf,[9] Jens Lykkesfeldt,[10] Myrte Merkestein,[2] Kei Sakamoto,[1] Birgitte Holst,[11,14] and Christoffer Clemmensen[1,16,*]

[1]Novo Nordisk Foundation Center for Basic Metabolic Research, Faculty of Health and Medical Sciences, University of Copenhagen, Copenhagen, Denmark
[2]Diabetes Pharmacology, Global Drug Discovery, Novo Nordisk A/S, Måløv, Denmark
[3]Diabetes and Metabolism Biology, Global Drug Discovery, Novo Nordisk A/S, Måløv, Denmark
[4]Obesity and NASH Research, Global Drug Discovery, Novo Nordisk, Lexington, MA, USA
[5]Center for Clinical Metabolic Research, Gentofte Hospital, University of Copenhagen, Copenhagen, Denmark
[6]Department of Clinical Medicine, Faculty of Health and Medical Sciences, University of Copenhagen, Copenhagen, Denmark
[7]Steno Diabetes Center Copenhagen, Herlev, Denmark
[8]Systems Biology and Target Discovery, AI and Digital Research, Novo Nordisk Research Center Oxford, Novo Nordisk A/S, Oxford, UK
[9]Research Chemistry, Global Research Technologies, Novo Nordisk A/S, Måløv, Denmark
[10]Section of Preclinical Disease Biology, Department of Veterinary and Animal Sciences, Faculty of Health and Medical Sciences, University of Copenhagen, Copenhagen, Denmark
[11]Department of Biomedical Sciences, Faculty of Health and Medical Sciences, University of Copenhagen, Copenhagen, Denmark
[12]Present address: Zealand Pharma A/S, Søborg, Denmark
[13]Present address: Novo Nordisk A/S, Søborg, Denmark
[14]Present address: Novo Nordisk Foundation, Hellerup, Denmark
[15]These authors contributed equally
[16]Lead contact
*Correspondence: chc@sund.ku.dk
https://doi.org/10.1016/j.xcrm.2025.101996

SUMMARY

Liver-expressed antimicrobial peptide 2 (LEAP2) is an endogenous antagonist and inverse agonist of the ghrelin receptor, countering ghrelin's effects on cell signaling and feeding. However, despite an emerging interest in LEAP2's physiology and pharmacology, its endocrine regulation remains unclear. Here, we report that plasma LEAP2 levels decrease significantly upon glucagon infusions during somatostatin clamps in humans. This effect is preserved in patients with obesity and type 2 diabetes while diminished following a hypercaloric diet and a sedentary lifestyle for 2 weeks. Additionally, insulin receptor antagonism offsets the upregulation of LEAP2 during the postprandial state in mice. Finally, insulin and glucagon receptor-expressing hepatocytes are the primary source of hepatic *LEAP2* expression, coinciding with a putative enhancer-like signature bound by insulin- and glucagon-regulated transcription factors at the *LEAP2* locus. Collectively, our findings implicate insulin and glucagon in regulating LEAP2 and warrant further investigations into the exact mechanisms orchestrating this endocrine axis.

INTRODUCTION

Ghrelin, an orexigenic peptide hormone requiring acylation by ghrelin-O-acyltransferase,[1] is primarily secreted from the stomach and acts as a starvation signal driving energy-seeking behavior and energy storage.[1,2] During periods of energy deficit, circulating ghrelin levels rise to prevent hypoglycemia.[3–5] In addition to inducing growth hormone (GH) secretion from the pituitary gland,[6] ghrelin promotes hunger by activating isoform 1a of the GH secretagogue receptor (GHS-R1a) on neuropeptide Y/Agouti-related protein (NPY/AgRP) neurons in the arcuate nucleus of the hypothalamus.[7,8] Furthermore, ghrelin inhibits insulin secretion from pancreatic β cells and stimulates glucagon secretion from pancreatic α-cells and—effects that may be mediated indirectly through the stimulation of somatostatin secretion from pancreatic δ-cells or hypothalamic neurons (glucagon only) expressing GHS-R1a.[9]

Liver-expressed antimicrobial peptide 2 (LEAP2) has been characterized as an endogenous peptide antagonist of the GHS-R1a by both acting as an inverse agonist against constitutive GHS-R1a activity and as a competitive antagonist of acyl ghrelin.[10–17] LEAP2 is reported to be mainly expressed in the liver and in the

small intestine of both mice and humans,[10] and LEAP2 infusion has been reported to reduce postprandial blood glucose excursions and food intake in both healthy individuals and individuals with obesity.[18,19] Consequently, LEAP2 may have therapeutic potential in obesity through the augmentation of the LEAP2/ghrelin balance and consequent reduction of GHS-R1a signaling. Gaining a more comprehensive understanding of LEAP2 biology, including delineation of the diverse regulatory mechanisms controlling circulating LEAP2 levels, has the potential to establish a strong foundation for the development of future LEAP2-based therapeutics.

Circulating LEAP2 is regulated by metabolic status where levels increase with a positive energy balance, in a direction opposite to that of ghrelin.[15] In humans, plasma LEAP2 levels have been shown to increase with body mass index,[15,20,21] blood glucose, and meal intake,[15,22] while decreasing with fasting, Roux-en-Y gastric bypass, and in the postprandial state of people who have undergone vertical sleeve gastrectomy.[15] In addition, plasma LEAP2 levels are positively associated with numerous metabolic parameters of obesity, including body fat percentage, waist-to-hip ratio, blood triglycerides, visceral adipose tissue volume, liver lipid content, fasting insulin, and homeostatic model assessment for insulin resistance.[15,20,23,24] Finally, LEAP2 has been associated with other obesity-related metabolic diseases, including metabolic-associated fatty liver disease (MAFLD).[23–25]

The fact that circulating LEAP2 levels increase after a meal in humans supports the notion that LEAP2 is upregulated by increased energy availability.[15,22] Our recent findings show that this response depends on the dietary challenge of interest and that the LEAP2 upregulation is associated with increased levels of liver glycogen and jejunal lipids.[26] Nevertheless, the underlying molecular mechanisms behind the metabolic and endocrine regulation of LEAP2 remain to be realized.

Upon secretion from the pancreatic α- and β cells, the catabolic and anabolic hormones, glucagon, and insulin, respectively, are crucial regulators of energy balance and usually exert counterregulatory effects on substrate metabolism in the fed and fasted states. Here, we hypothesized that glucagon and insulin might play key roles in regulating LEAP2. We demonstrate that LEAP2 levels in the circulation decrease significantly during pancreatic somatostatin clamps with supraphysiological glucagon infusions in humans. Additionally, the postprandial upregulation of LEAP2 is diminished by insulin receptor antagonism in mice. Furthermore, single-cell RNA sequencing (scRNA-seq) and single-nucleus RNA sequencing (snRNA-seq) analyses of our constructed human liver atlas reveal that hepatocytes are the main cell type of hepatic *LEAP2* expression with high co-expression of *GCGR* and *INSR*. This co-expression aligns with a putative enhancer-like signature at the *LEAP2* locus in the liver, bound by insulin and glucagon-regulated transcription factors. Collectively, our results suggest that both glucagon and insulin regulate LEAP2.

RESULTS

Circulating LEAP2 levels decrease upon supraphysiological glucagon infusions in humans

To investigate the effect of glucagon and a hypercaloric diet on LEAP2 regulation, 20 healthy individuals were recruited for a dietary hypercaloric intervention study. The individuals were exposed to pancreatic somatostatin clamps with glucagon infusions emulating fasting (0.6 ng × kg^{-1} × min^{-1}) and supraphysiological (4.0 ng × kg^{-1} × min^{-1}) levels on three occasions: prior to and immediately after the 2-week hypercaloric dietary intervention and after an 8-week recovery period (day A, B, and C, respectively) (Figure 1A). The individuals reached supraphysiological glucagon concentrations during the infusion period (Figure 1B), while the pancreatic somatostatin clamp efficaciously maintained low C-peptide levels (Figure 1C). The dietary intervention did not change plasma LEAP2 levels prior to the clamp (Figure 1D). However, at all three experimental days, plasma LEAP2 levels decreased significantly upon high plasma glucagon concentrations (Figures 1D and 1E). Interestingly, the extent by which LEAP2 levels decreased in response to high glucagon infusions depended on the experimental day. The decrease in LEAP2 levels upon 1 and 2 h of supraphysiological glucagon was significantly impaired by the dietary intervention compared to baseline measurements (Figures 1D and 1E), whereas sensitivity was restored after recovery from the hypercaloric dietary intervention (Figures 1D and 1E). Individuals experiencing the greatest relative glucagon increases during the clamp also tended to be the ones with the highest decrease in plasma LEAP2 levels (Figure S1). Plasma LEAP2 levels prior to the initiation of the clamp tended to correlate positively with plasma insulin, but not C-peptide, glucagon, BMI, or glucose (Figure S2). To contextualize these findings, we utilized data from an experimental animal study (GEO: accession number GSE110673), where lean mice fed a normal chow diet with implanted micro-osmotic pumps were infused with glucagon for 7 days. Following treatment with glucagon in this experiment, mice tended to decrease their hepatic *Leap2* mRNA levels compared to nontreated controls, although this did not reach statistical significance (Figure S3A). Treatment with a long-acting glucagon analog did not affect *Leap2* expression in diet-induced obese (DIO) mice (Figure S3B).

To determine whether the effect on LEAP2 observed during the glucagon infusions in healthy individuals (Figures 1A–1E) was replicated in patients with obesity and/or type 2 diabetes, we analyzed circulating LEAP2 levels from these patient groups during infusions with supraphysiological glucagon (Figures 1F and 1G). Importantly, patients with obesity (Figure 1H) and type 2 diabetes (Figure 1I) also presented with decreased plasma LEAP2 levels following 1 h of supraphysiological glucagon infusions (Figures 1H and 1I, time point 60 min), which tended to recover after the infusion period (Figures 1H and 1I, time point 120 min). These data suggest that LEAP2 levels in the circulation are affected by glucagon infusions in humans and that the effect is maintained in patients with obesity and/or type 2 diabetes, while diminished by a hypercaloric diet.

Insulin receptor antagonism offsets postprandial upregulation of hepatic *Leap2* mRNA expression and plasma LEAP2 levels in mice

To assess the regulation of LEAP2 by insulin, mice were administered a mixed meal by oral gavage in the presence or absence of a subcutaneously (s.c.) dosed, selective insulin receptor antagonist, S961 (Figure 2A). Prior to the meal challenge, mice

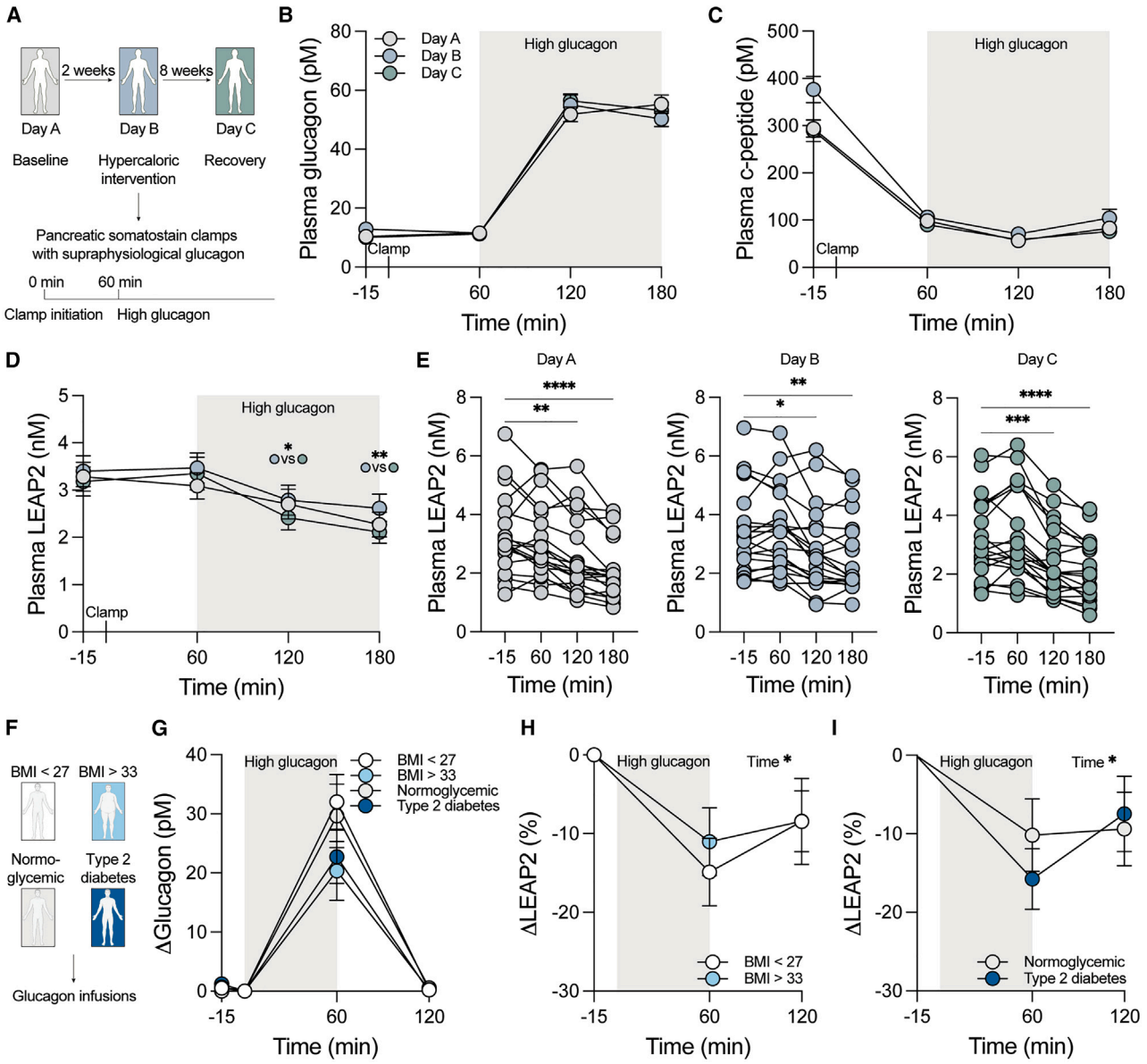

Figure 1. Plasma LEAP2 levels decrease during supraphysiological glucagon infusions in pancreatic somatostatin clamps in healthy individuals and in patients with obesity and type 2 diabetes

(A) Schematic of the experimental design. Twenty healthy individuals were recruited for the 2-week hypercaloric dietary intervention. At three identical experimental days (day A: baseline [gray], day B: after a 2-week hypercaloric diet [light blue], day C: after an 8-week recovery [green]), and following a 10-h overnight fast, the participants were subjected to a pancreatic somatostatin clamp.

(B and C) Plasma glucagon (B) or C-peptide (C) levels before the somatostatin clamp with basal insulin and glucagon infusions (−15 min), before infusions with supraphysiological glucagon (60 min), and after 1 (120 min) and 2 h (180 min) of supraphysiological glucagon infusions. The initiation of the clamp is indicated on the x axis.

(D and E) Plasma LEAP2 levels from each experimental day during the pancreatic somatostatin clamps with high glucagon infusions.

(F) Schematic of the experimental design. Individuals with BMI below 27 (white), above 33 (turquoise), normoglycemia (light gray), or type 2 diabetes (dark blue) were subjected to 1 h glucagon infusions.

(G) Relative changes in plasma glucagon levels (from time point 0 min) before glucagon infusions (−15 min), after 1 h of supraphysiological glucagon (60 min), and after 1 h of recovery (120 min).

(H and I) Relative changes in plasma LEAP2 levels (from time point −15 min) after 1 h of supraphysiological glucagon infusions and after 1 h of recovery.

Data are presented as mean +/- SEM. Statistics in (D) by repeated measures two-way ANOVA, multiple comparisons corrected for multiple testing using Tukey method. Statistics in (E) by repeated measures one-way ANOVA, Dunnett's multiple comparisons tests. Statistics in (H) and (I) by repeated measures two-way ANOVA. $p < 0.05$, *$p < 0.01$, **$p < 0.001$, ***$p < 0.0001$, ****.

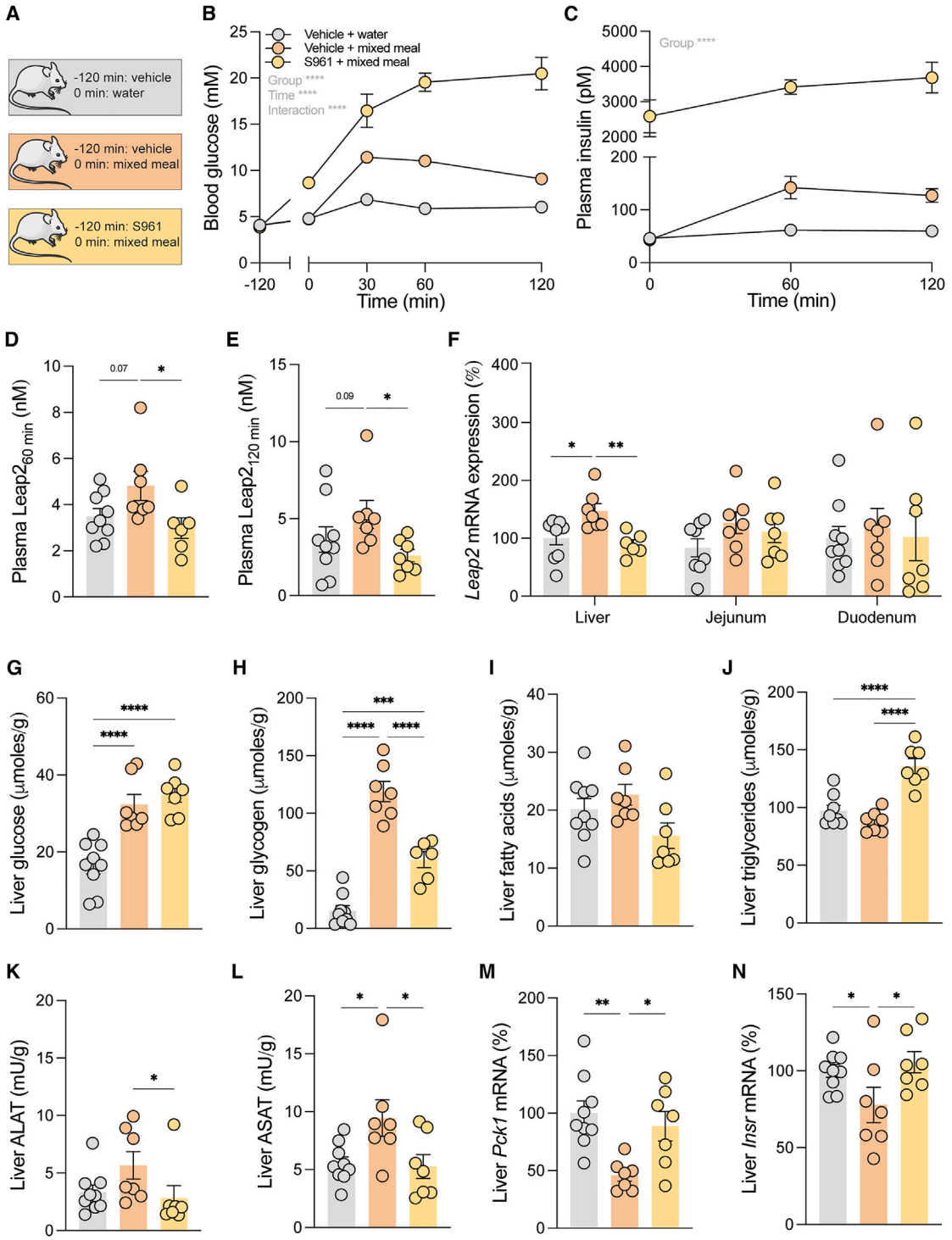

Figure 2. Insulin is required for the meal-induced upregulation of hepatic *Leap2* mRNA expression and plasma LEAP2 levels in lean mice

(A) Schematic of the experimental *in vivo* study for examining the role of insulin in the LEAP2 response after administration of a mixed meal. The three different groups of mice were those that received an s.c. vehicle dosage 2 h prior to an oral water challenge (gray), those that received an s.c. vehicle dosage prior to an oral mixed meal challenge (orange), and those that received an s.c. insulin receptor antagonist (S961) prior to a mixed meal challenge (yellow).

(B and C) Blood glucose profiles (B) and plasma insulin levels (C) during the intervention.

(D and E) Plasma LEAP2 levels 1 (D) and 2 h (E) post oral gavage.

(F) Liver (left), jejunal (middle), and duodenal (right) *Leap2* mRNA levels in response to the intervention.

(legend continued on next page)

pre-dosed with S961 had significantly increased blood glucose and plasma insulin levels compared to mice that received an isovolumic vehicle injection (Figures 2B and 2C), confirming the insulin receptor antagonistic effect. In the groups receiving s.c. vehicle, oral mixed meal vs. water dosing also significantly increased blood glucose and plasma insulin levels (Figures 2B and 2C), emphasizing that the experimental paradigm is suitable for studying postprandial hormonal regulation of LEAP2. We next asked if the circulating LEAP2 levels were affected by dosing of the insulin receptor antagonist. Mice that were pre-dosed with S961 prior to a mixed meal had significantly lower plasma LEAP2 levels 60 and 120 min post mixed-meal dosing than mice dosed with vehicle and a mixed meal (Figures 2D and 2E). Mixed meal vs. water dosing increased hepatic *Leap2* mRNA expression, whereas this postprandial effect on hepatic *Leap2* mRNA expression was completely abolished by pre-dosing the mice with the insulin receptor antagonist (Figure 2F). In the small intestine, however, we observed only a tendency toward increased jejunal *Leap2* mRNA expression in mice in response to a mixed meal, an effect that was even further attenuated in the duodenum of these mice (Figure 2F). Surprisingly, however, exogenous intraperitoneal insulin injections, causing pronounced hypoglycemia, were insufficient to increase plasma LEAP2 levels in both chow-fed lean mice and DIO mice fed a high-fat high-sucrose diet (Figure S4).

Aiming at further characterizing the *in vivo* intervention to contextualize the findings that postprandial, hepatic *Leap2* upregulation was completely blunted by insulin receptor antagonism, we chose to profile the metabolic status of the livers of these mice. Mice receiving a mixed-meal challenge had significantly greater hepatic glucose levels (Figure 2G) and accumulated more hepatic glycogen (Figure 2H) than mice receiving oral water dosing. While there was no significant difference in hepatic glucose levels between S961 and vehicle-dosed mice receiving a mixed meal, hepatic glycogen levels were significantly decreased in mice dosed with a mixed meal and treated with S961 vs. vehicle (Figures 2G and 2H). We did not detect any change in liver fatty acids and triglyceride levels in response to a mixed meal, when compared to mice that were injected with vehicle (Figures 2I and 2J). However, mice administered a mixed meal and treated with S961 vs. vehicle had significantly decreased fatty acids levels and increased triglycerides in the liver (Figures 2I and 2J). While there was a tendency toward an increase in the liver enzymes alanine transaminase (ALAT) and aspartate transaminase (ASAT) with the mixed meal vs. water challenge, the levels of these enzymes were significantly decreased in mice dosed with a mixed meal treated with S961 vs. vehicle (Figures 2K and 2L). Finally, we also sought to control for the effect of insulin receptor antagonism specifically at the liver level (i.e., genes regulated by insulin) and found significantly decreased phosphoenolpyruvate carboxy kinase 1 (*Pck1*) and insulin receptor (*Insr*) mRNA expression in the group of mice that received a mixed meal vs. water and that this effect was reversed by S961 dosing (Figures 2M and 2N).

Taken together, these data suggest that the action of insulin is required for the postprandial upregulation of LEAP2, while exogenous insulin is insufficient to increase plasma LEAP2 levels.

Casein protein does not affect LEAP2 levels in mice

The role of dietary carbohydrates and fats has previously been studied in the context of LEAP2 regulation.[26] It remains to be determined if dietary protein affects LEAP2. To study this, we challenged mice with either oral casein or water and assessed plasma LEAP2 levels 1 and 2 h post dosing in lean C57BL/6J mice (Figure 3A). This intervention caused no major changes in blood glucose or plasma insulin levels (Figures 3B and 3C). We detected no significant changes in plasma LEAP2 levels, but observed a trend toward increased levels in mice receiving casein compared to those receiving water at 1 h post dosing (Figures 3D and 3E). No significant changes in *Leap2* mRNA levels between the two groups were observed in the liver (Figure 3F) or jejunum (Figure 3G). Casein gavage did not change liver metabolic parameters, including glucose (Figure 3H), glycogen (Figure 3I), fatty acids (Figure 3J), triglycerides (Figure 3K), ALAT (Figure S5A), or ASAT levels (Figure S5B). Taken together, these results indicate that the protein component of a mixed meal, casein, does not affect plasma LEAP2 levels or hepatic and small intestine *Leap2* gene expression.

Insulin and glucagon-regulated transcription factors bind a putative proximal enhancer-like structure at the transcriptional start site of *LEAP2* in a liver-filtered ChIP-Atlas

To gain further insights into how insulin and glucagon might regulate LEAP2, we pursued potential genomic evidence to support or challenge our studies in humans and mice. When human *LEAP2* expression was examined by bulk tissue RNA sequencing (RNA-seq) in the Genotype-Tissue Expression (Gtex) portal, the liver was the main organ expressing *LEAP2*, while certain brain regions, such as the cerebellum, and the small intestine also presented with high *LEAP2* mRNA expression (Figure S6). We thus examined available liver-specific data from the chromatin immunoprecipitation (ChIP)-Atlas to better understand the genomic architecture at the *LEAP2* locus. Around the *LEAP2* transcriptional start site, chromatin appeared accessible for transposons and sensitive to DNase treatment, as visualized by assay for transposase-accessible chromatin using sequencing (ATAC-seq) and DNase sequencing (DNase-seq) tracks, respectively (Figure 4A). DNA at these open chromatin regions was marked as hypomethylated regions by bisulfite sequencing (bisulfite-seq) (Figure 4A). H3K27ac and H3K4me1/2/3 histone marks, indicative of enhancer and promoter regions, overlapped the regions with supposedly open chromatin around the *LEAP2* gene, while the DNA at this region did not appear to be characterized by

(G–L) Hepatic glucose (G), glycogen (H), fatty acid (I), triglyceride (J), ALAT protein (K), and ASAT protein (L) levels in response to the intervention.
(M and N) Hepatic *Pck1* (M) and *Insr* (N) mRNA levels in response to the intervention.
Data are presented as mean +/- SEM. Statistics in (B) and (C) by mixed-effects models. Statistics in (D), (E), (F), (K), (M), and (N) by Kruskal-Wallis and uncorrected Dunn's test. Statistics in (G), (H), (J), and (L) one-way ANOVA and uncorrected Fisher's LSD test. $p < 0.05$, $^{*}p < 0.01$, $^{**}p < 0.001$, $^{***}p < 0.0001$, ****.

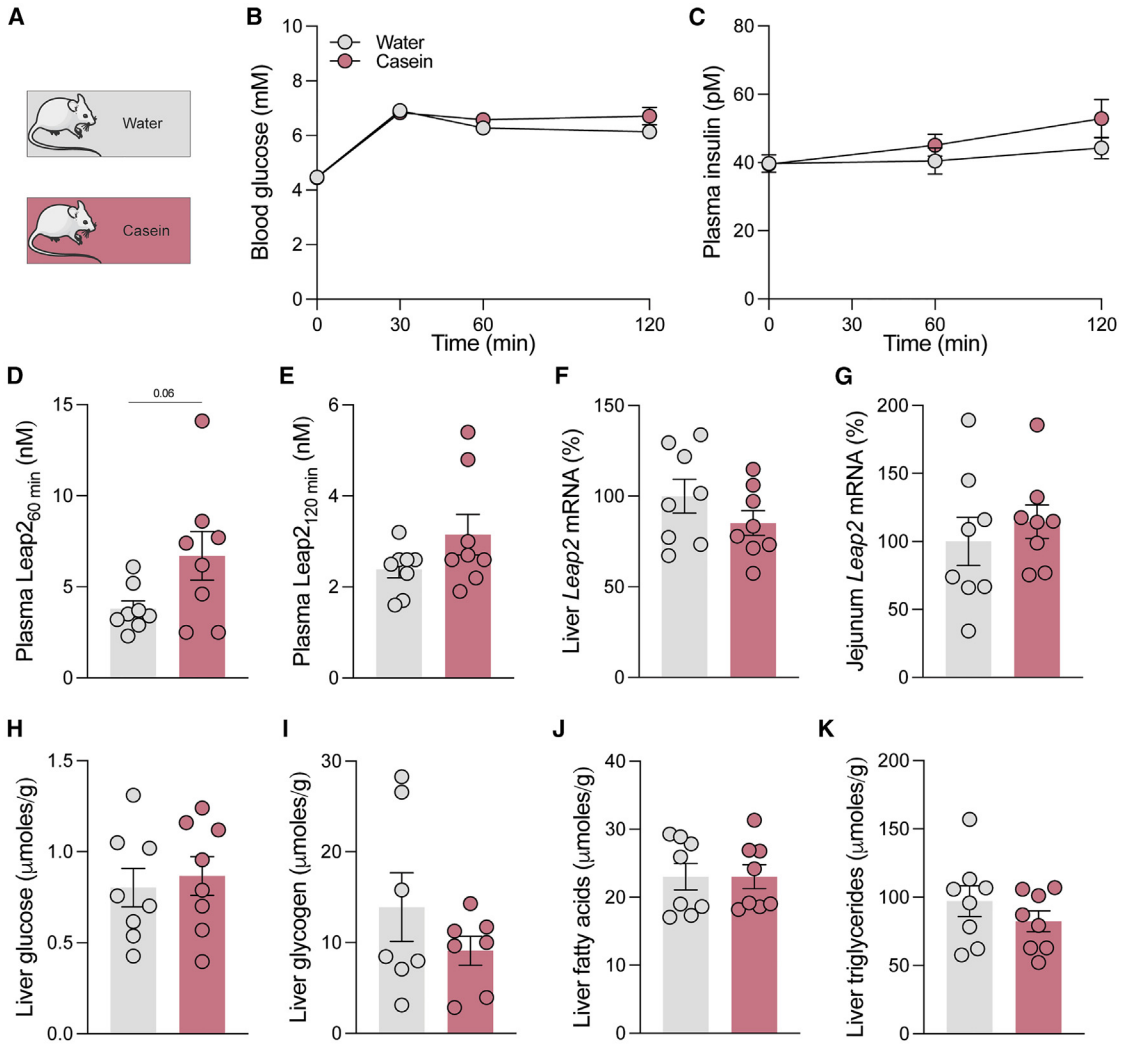

Figure 3. The protein component of the mixed meal, casein, does not regulate LEAP2

(A) Schematic illustration. To examine the potential role of casein on LEAP2 regulation, mice were fasted for 16 h prior to a casein or water challenge by oral gavage.

(B and C) Blood glucose profiles (B) and plasma insulin levels (C) from mice orally dosed with isovolumic water (gray) or 16% kcal/kg casein (red) (matching protein constituent by kcal% from the mixed-meal dosing in Figure 2).

(D–G) Plasma LEAP2 levels 1 (D) and 2 h (E) post oral gavage, and *Leap2* mRNA levels of liver (F) and jejunum (G) from the mice.

(H–K) Hepatic glucose (H), glycogen (I), fatty acids (J), and triglyceride (K) levels from the mice.

Data are presnted as mean +/- SEM. Statistics in (D) by unpaired t test.

H3K9me1 repressor marks (Figure 4A). Importantly, the ENCODE Candidate *cis*-regulatory elements (cCREs) track from the UCSC Genome Browser supported these findings by marking these same regions upstream and at the *LEAP2* transcriptional start site as proximal enhancer-like signatures (Figure 4A, orange). The cCREs track annotated other regions downstream of the *LEAP2* gene within the last exon of the ATF4 gene as distal enhancer-like signatures (Figure 4A, yellow). Interestingly, filtering data for hepatocytes specifically revealed a similar DNase and ATAC-seq pattern with similar histone marks just proximal to the transcriptional start site of *LEAP2* (Figure S7). At these enhancer-like structures, we used all the publicly available liver-specific ChIP data in the ChIP-Atlas to ask which regulatory proteins bind to this putative *LEAP2* enhancer. Indeed, most regulatory proteins around this genomic locus bind at this specific region, as visualized by the transcription factor binding density track (Figure 4A).

Most importantly, when filtering for liver ChIP sequencing (ChIP-seq) data, multiple insulin and glucagon-regulated transcription factors, such as specificity protein 1 (SP1), Forkhead box protein O1 (FOXO1), and some from the Forkhead box protein A (FOXAs) and hepatocyte nuclear factor (HNFs) families, bind the proximal enhancer-like signature just upstream of the *LEAP2* transcription start site (Figure 4B). Although a similar proximal *LEAP2* enhancer-like signature was evident when examining all data from the digestive tract in the human

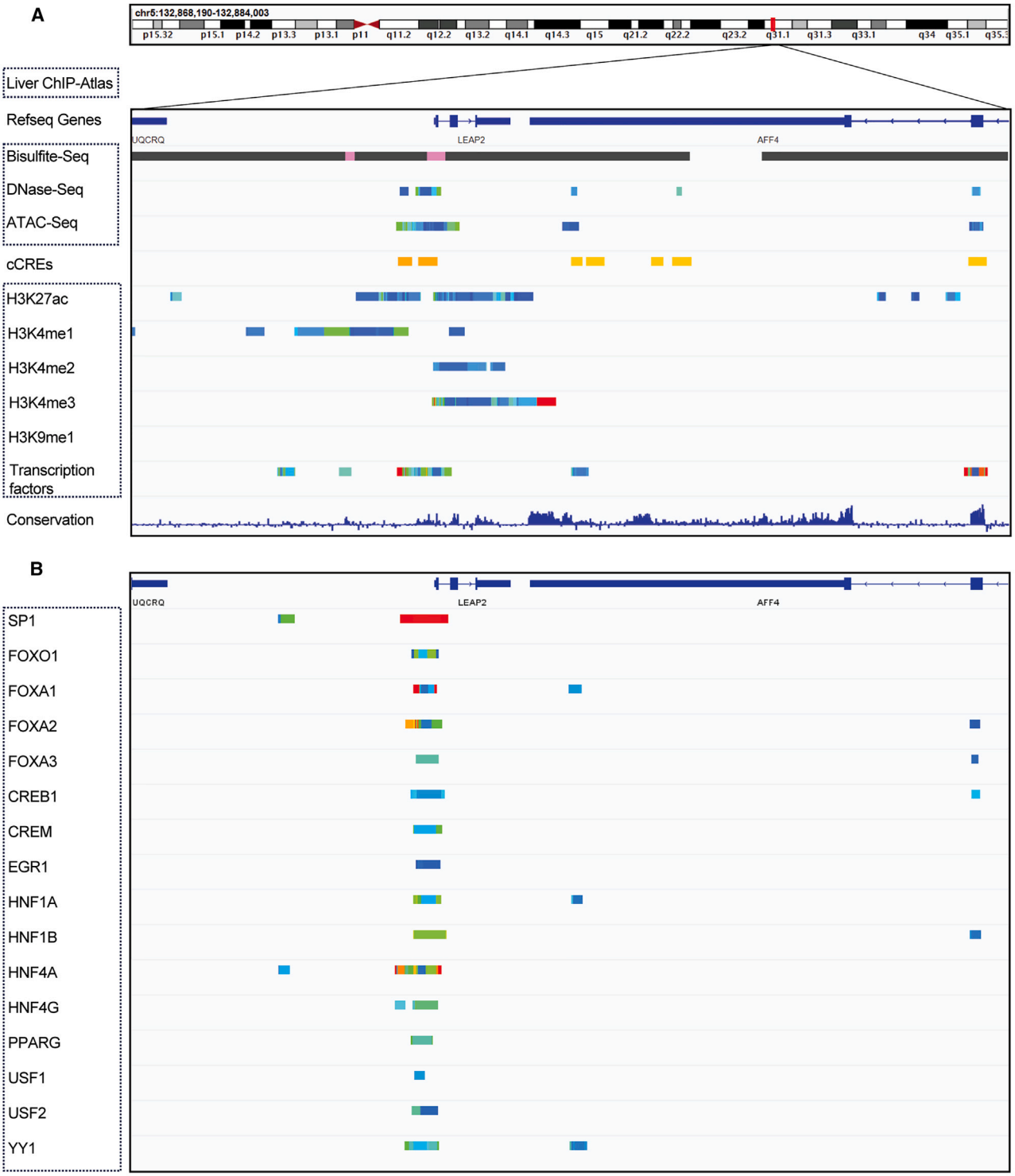

Figure 4. Insulin and glucagon-regulated transcription factors bind a putative proximal enhancer-like structure at the transcriptional start site of *LEAP2* revealed by hepatic data from the human ChIP-Atlas

(A) Integrative Genomics Viewer (IGV) from Hg38 at position chr5; 132,868,190-132,884,003 with summarized dense tracks of Refseq genes and liver-filtered ChIP-Atlas data of bisulfite-seq (pink indicates hypomethylated region, black indicates hypermethylated region), ATAC-seq, DNase-seq, H3K27ac, H3K4me1, H3K4me2, H3K4me3, and transcription factor binding. All ChIP-seq data are color-coded based on the amount of data reporting a count at a given site from a ChIP-seq experiment deposited in the ChIP-Atlas and classified as a liver sample (red indicates high number of counts, green indicates low number of counts).

(legend continued on next page)

ChIP-Atlas, this genomic locus did not seem to be occupied by the same insulin and glucagon-regulated transcription factors in this tissue and in intestine-derived cell types (Figure S8). Of note, using liver-filtered data in the mm10 mouse assembly of the ChIP-Atlas, we identified similar chromatin characteristics and transcription factor binding landscapes as in the human hg38 assembly, although not identical (Figure S9).

Human hepatocytes are the main source of hepatic *LEAP2* expression at the single-cell level

To examine which specific hepatic cell types are the main source of *LEAP2* expression in the liver, we generated a comprehensive liver cell atlas by integrating six independent studies of human hepatic snRNA-seq and scRNA-seq data (Figures 5A–5C). Hepatocytes, cholangiocytes, and stellate cells all displayed pronounced *LEAP2* expression (Figure 5D), while hepatocytes had the highest mean *LEAP2* expression and largest fraction of cells expressing *LEAP2* across the 8 major liver cell types (Figures 5D and 5E). Notably, these cell types also represented the groups of cells that had the highest expression levels of *GCGR* and *INSR* (Figure 5E). In both snRNA-seq studies with greatest hepatocyte coverage (Figure 5C), *LEAP2* mean transcript levels were significantly increased in hepatocytes from individuals with metabolic dysfunction-associated steatohepatitis (MASH) compared to that of hepatocytes from individuals without MASH (Figure 5F). Together, these data highlight the metabolically active hepatocytes as the primary source of hepatic *LEAP2* expression.

Insulin treatment decreases *Leap2* mRNA expression in liver cells

The finding that hepatocytes highly express *LEAP2* mRNA in the liver prompted us to investigate if the insulin receptor-dependent upregulation of hepatic *Leap2* mRNA expression in response to nutrients (Figure 2) is caused by the direct action of hepatocyte insulin signaling. To examine this, we stimulated overnight-fasted primary mouse hepatocytes with insulin, glucose, or S961 alone or in combination and measured *Leap2* mRNA content. To ensure that our batches of primary hepatocytes responded to insulin treatment, we measured *Pck1* mRNA expression upon insulin treatment as well as the phosphorylation state of Akt 1/2/3 upon titration with insulin or S961 with fixed insulin concentration (Figures 6A and 6B). Surprisingly, direct simulation with insulin alone or in combination with glucose significantly decreased *Leap2* mRNA expression compared to a control treatment (Figure 6B). To assess whether the downregulation of *Leap2* could be mediated by a negative feedback loop from insulin-induced Leap2 secretion from the hepatocytes, we measured LEAP2 protein levels in the cell medium. Although there appeared to be no significant difference under these same conditions, the concentrations detected by ELISA were low with high intra-assay variation (results not shown, LEAP2 concentration range: 0.06–0.11 nM).

To substantiate our results from primary mouse hepatocytes, we cultured human HepG2-insulin-like growth factor 1 receptor (IGF1R)-knockout (KO) cells (IGF1R was knocked out to mimic human hepatocytes) followed by insulin stimulation or no stimulation and performed bulk RNA-seq. The two conditions were separated by supervised principal component analysis, covering more than 74% variance in our dataset (Figure 6C), and when comparing transcriptomes in the absence or presence of insulin stimulation, 8,438 genes were significantly differentially expressed (Figure 6D). Of note, also a supervised *k*-means clustering approach clustered our samples dependent on condition (Figure 6C). Importantly, HepG2-IGF1R-KO cells had significantly decreased *LEAP2* mRNA expression (log2FC = −0.7933) after 3 nM human insulin stimulation (Figure 6E), consistent with insulin stimulation of mouse hepatocytes. In contrast, glucagon stimulation of mouse hepatocytes increased *Leap2* expression (Figure S10A). Having established that our *in vitro* systems of mouse and human liver cells did not support the idea of insulin directly upregulating hepatic *Leap2* mRNA expression, we next investigated the role of direct insulin stimulation at the intestinal level on *LEAP2* mRNA expression using mouse and human jejunal organoids. We tested the effect of glucose and oleic and linoleic acids on *LEAP2* expression in mouse and human jejunal organoids alone or in the presence of insulin and S961. In human jejunal organoids, glucose and fatty acids alone did not upregulate *LEAP2*, but *LEAP2* mRNA levels were significantly increased by the nutrients in combination with insulin. This increase in *LEAP2* mRNA levels was abolished in the presence of S961 (Figure S10B). In mouse jejunal organoids, we observed no significant *Leap2* mRNA upregulation by glucose and fatty acids (Figure S10C).

Together, these *in vitro* findings add to the complexity of the interplay of glucagon, insulin, and LEAP2 and suggest that the effects observed *in vivo* are unlikely to occur through the direct stimulation of hepatocytes, although constituting the cell type in the liver expressing *LEAP2* the most.

DISCUSSION

The pharmacological potential of the GHS-R1a antagonist and inverse agonist, LEAP2, has gained recent attention. However, its endogenous regulation remains incompletely understood. Here, we examined how hormones from the endocrine pancreas regulate LEAP2. We observed that plasma LEAP2 levels decrease upon supraphysiological glucagon infusions during pancreatic somatostatin clamps in healthy individuals and that a 2-week hypercaloric dietary intervention impaired the LEAP2 plasma response to glucagon infusions. A similar pattern was identified in patients living with obesity and/or type 2 diabetes. Furthermore, using insulin receptor antagonism, we found that the action of insulin is necessary to increase postprandial hepatic *Leap2* expression and plasma LEAP2 levels associated with a

ENCODE candidate *cis*-regulatory elements (orange indicates proximal enhancer-like signatures, yellow indicates distal enhancer-like signatures) and PhyloP conservation (the higher the peak at a site, the less likely it is to observe a given site under a null hypothesis of neutral evolution) tracks from the UCSC Genome Browser also indicated (please refer to STAR Methods).
(B) IGV view at the same position and in the same assembly as in (A) with liver-filtered ChIP-Atlas data of indicated insulin and glucagon-regulated transcription factors.

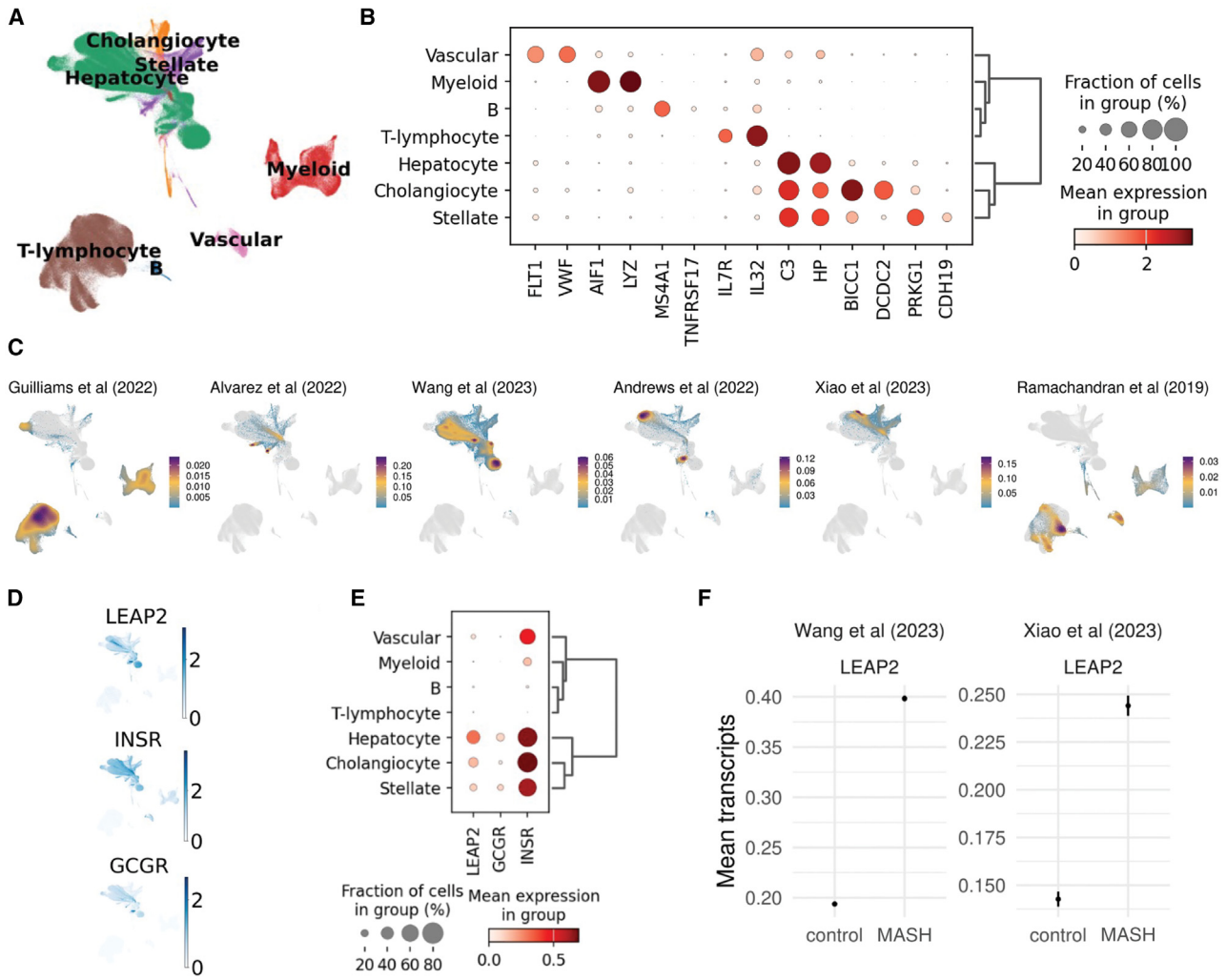

Figure 5. *LEAP2* gene expression is enriched to hepatocytes, cholangiocytes, and stellate cells in the human liver

(A) Liver cellular landscape. Uniform manifold approximation and projection (UMAP) embedding of 545,869 cells from 93 samples along 6 cohorts.

(B) Cell type-specific gene expression for the 8 major liver cell types.

(C) Cell density distribution for each of the integrated cohorts.

(D and E) Co-expression of *LEAP2*, *INSR*, and *GCGR* genes.

(F) *LEAP2* is upregulated in MASH hepatocytes, Wilcoxon signed-rank tests $p < 0.001$.

mixed meal in mice. Collectively, these findings suggest that glucagon and insulin could exert opposite effects on LEAP2.

Both glucagon and insulin are reported to affect expression and circulating levels of ghrelin,[27] although some studies report no direct effect of these hormones on ghrelin regulation.[28–33] Considering that ghrelin and LEAP2, like glucagon and insulin, are inversely regulated by energy balance,[34] we sought to determine if LEAP2 was regulated by these hormones. Our findings suggest that, as with energy storage, insulin and glucagon may exert counterregulatory effects on LEAP2 regulation by stimulating and inhibiting its expression and/or secretion, respectively. However, the fact that no correlation was found between fasting concentrations of LEAP2, insulin, C-peptide, and glucagon levels in the human subjects could argue against a potential regulation by these hormones in the fasted state. Moreover, in the postprandial state, circulating LEAP2 was reported not to correlate with insulin in healthy individuals and individuals with obesity upon mixed meal ingestion (730 and 600 kcal,[15] respectively), despite postprandial increases in LEAP2. Here, we extend these correlational findings and study direct effects of manipulating insulin receptor signaling and glucagon levels to understand their impact on LEAP2 regulation.

Interestingly, LEAP2 is reported to antagonize the insulinostatic effect of ghrelin *in vitro*,[35] and an N-terminal LEAP2 fragment, $LEAP2_{38-47}$, has insulinotropic properties in human pancreatic islets.[36] LEAP2 has also been reported to increase insulin secretion during fasting in humans. In the same work, LEAP2 was also found to increase glucagon levels in both the fasted and postprandial state—an increase speculated to counteract the glucose-lowering effect of LEAP2.[18] Thus, the

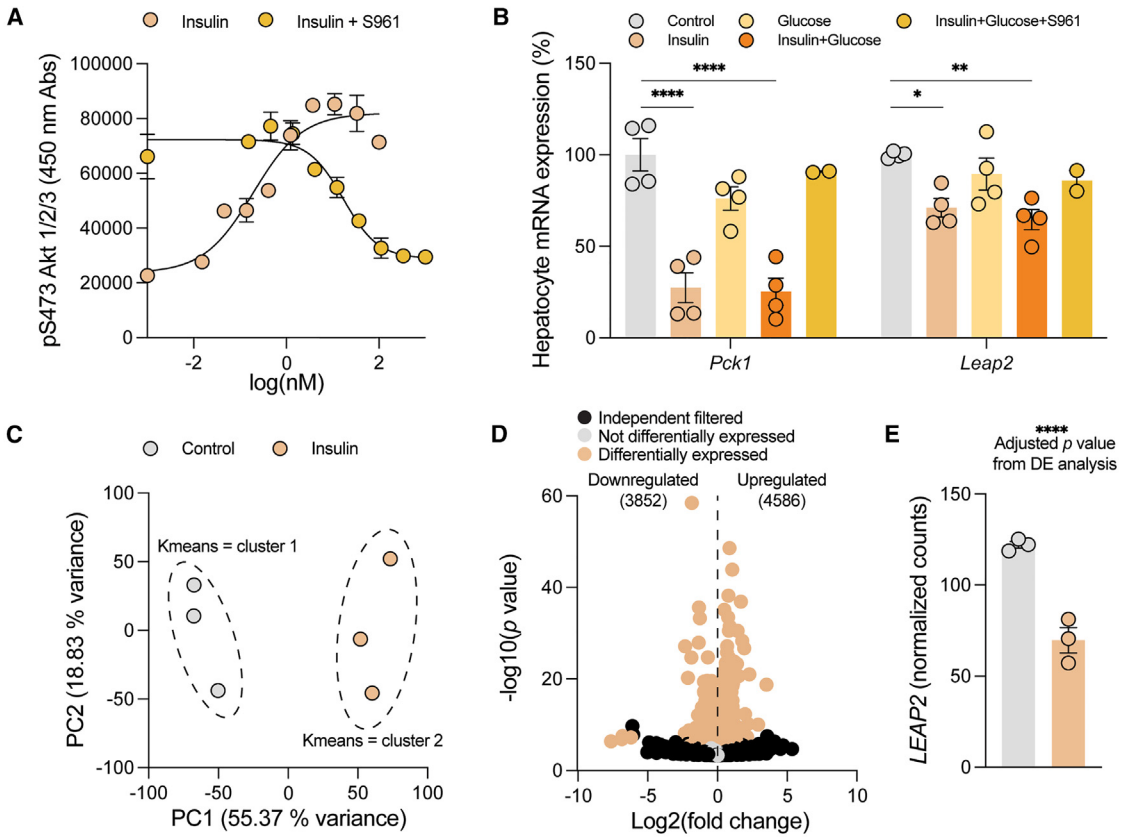

Figure 6. *LEAP2* mRNA levels decrease in mouse primary hepatocytes and HepG2-IGF1R-KO cells upon insulin stimulation *in vitro*

(A) Representative graph of phosphorylated S473 (pS473) Akt1/2/3 signals after surefire analysis of a mouse primary hepatocyte batch stimulated with a 2-fold titration of 100 nM human insulin (orange) or a 2-fold titration of 1000 nM S961 and a fixed human insulin concentration of 10 nM (yellow) for 15 min to test for insulin responsiveness. Data points represent technical replicates.

(B) *Pck1* (left) and *Leap2* (right) and mRNA levels from mouse primary hepatocytes that were fasted overnight and stimulated for 4 h with either 3 nM human insulin, 20 mM glucose, 30 nM S961, in combination or alone, or with a control solution of starvation medium containing 1% human serum albumin as indicated. Data from four pooled technical replicates from two independent biological replicates.

(C) Supervised principal component analysis plot of normalized counts from bulk RNA-seq-yielded transcriptomes of HepG2-IGF1R-KO cells incubated in DMEM with 10% FBS (normal medium, control) with no stimulation (gray) and with 18 h 3 nM insulin stimulation (orange). Overlay of cluster designations from a *k*-means clustering with $k = 2$. Data from normalized counts of three independent experiments with averages from three technical repeats per experiment.

(D) Volcano plot of same samples as in (C) with each gene color-coded according to the adjusted p value < 0.05 (orange) or ≥ 0.05 (gray). Black data points indicate genes that are independently filtered during differential gene expression analysis.

(E) Normalized counts of *LEAP2* from same samples as in (C) and (D).

Data in (A), (B), and (E) are presented as mean +/- SEM. Statistics in (B) by ANOVA. Statistics in (E) from differential gene expression analysis (please refer to STAR Methods). $p < 0.0001$, ****.

hormones may affect each other's regulation, potentially in response to blood glucose levels or overall energy status (Figure S11).

Here, we found that blocking the insulin receptor with a selective receptor antagonist resulted in significantly lower liver glycogen levels, yet significantly higher liver triglyceride levels, in mice fed a mixed meal. The fact that glycogen levels, and not *Leap2* expression, increased in mice dosed with S961 and a mixed meal vs. vehicle and water argues against direct regulation of LEAP2 by local substrate availability. Furthermore, LEAP2 has been reported to increase with augmented hepatic lipid deposition,[23] which is in contrast to our findings. Thus, rather than local energy availability, our study suggests that LEAP2 responds to insulin-dependent signaling cascades upstream of the effects of insulin on energy availability. For a mixed meal, this signal is likely mediated by increased availability of carbohydrates, which represents the strongest stimulus for insulin secretion, since we show that neither casein (the main protein component of the mixed meal) nor dietary lipid[26] affects hepatic *Leap2* mRNA expression in mice.

Given that the endocrine pancreas discharges its content into the hepatic portal vein, the liver is the first organ exposed to both insulin and glucagon, which play an essential role in liver metabolism. As previously discussed, our human and mouse studies also suggest that these hormones may play a key role in LEAP2 regulation. In the liver, we found human hepatocytes to be the

major source of hepatic *LEAP2* mRNA expression by analyzing and integrating publicly available scRNA-seq and snRNA-seq data. In contrast to our *in vivo* findings, we found that insulin stimulation caused downregulation of *Leap2* mRNA expression *in vitro*. This discrepancy could be explained by several factors. First, it is possible that the insulin-dependent increase in *Leap2* mRNA expression associated with a mixed meal *in vivo* arises from insulin-dependent actions that reach the liver through a CNS-liver axis implicating the autonomous nervous system. Indeed, it has been suggested that insulin partially exerts control over hepatic glucose production through central mechanisms in rodents,[37–40] although studies in dogs indicate that inhibition of hepatic glucose production is attributable to insulin's direct effect on the liver.[41,42] Second, it may be that our *in vivo* findings do reflect a direct insulin-dependent effect on the liver to upregulate *Leap2* mRNA levels in response to a mixed meal, but that this effect is the result of a complex regulation requiring additional circulating factors or additional cell types in the liver, which are absent in the *in vitro* culturing of hepatocytes and HepG2-IGF1R-KO cells. Third, the effect of insulin on *Leap2* mRNA upregulation may be influenced by timing and dosing, which can vary depending on the system and are not easily replicated in *in vitro* models. All of these factors might be crucial for insulin-mediated upregulation of LEAP2 in response to a mixed meal *in vivo*. However, their absence and interactions are not accounted for *in vitro*, which limits our understanding of how insulin regulates LEAP2.

Despite being the organ with the highest expression of *Leap2* mRNA, LEAP2 protein levels were undetectable by ELISA in both homogenized mouse livers and cell lysates of mouse hepatocyte, while LEAP2 protein levels could be detected in the small intestine of mice.[26] This could suggest that LEAP2 is secreted more rapidly from liver cells compared to LEAP2 secretion in intestinal cells. It is thus possible that this rapid secretion of LEAP2 exhibits paracrine actions on liver cells influencing *Leap2* mRNA expression through receptor-mediated pathways, thereby explaining the downregulation of LEAP2 in hepatocytes upon insulin stimulation. However, the fact that LEAP2 levels in the cell medium did not differ across the groups could argue against such a potential negative feedback loop, although the low levels (0.06–0.11 nM) detected make it difficult to conclude on this matter. Furthermore, because ghrelin has been shown to inhibit liver *LEAP2* expression through a GHS-R1a-AMPK-dependent pathway in hepatocytes,[17] it also seems unlikely that LEAP2 could participate in a negative feedback loop through GHS-R1a, currently the only putatively identified LEAP2 receptor in the liver.

Here, we failed to detect an increase in small intestine *Leap2* expression in response to a mixed meal in mice. This is in contrast to previous findings by Gradel et al.[26] and might be explained by the higher blood glucose levels achieved upon mixed-meal dosing compared to our study. No significant upregulation was observed in mouse jejunal organoids, but human organoids showed elevated *LEAP2* expression when stimulated both by nutrients and insulin. This species-specific difference calls for further research into the intestinal regulation of LEAP2 associated with the luminal presence of nutrients. In continuation, in this study, we provide bioinformatic evidence that both tissues and cells from the digestive tract and liver-derived cells contain a putative *LEAP2* enhancer just upstream to the *LEAP2* transcriptional start site. As we characterized this genomic locus, we identified insulin and glucagon-regulated transcription factors that bound differentially to the *LEAP2* proximal enhancer-like signature depending on tissue. The fact that many of these bind to the liver *LEAP2* genomic locus, but not to the putative *LEAP2* enhancer in digestive tract tissues and cells, suggest that *LEAP2* expression is regulated rather differently by insulin and glucagon in these tissues, which fit our observations of postprandial insulin-dependent *Leap2* upregulation in the liver but not in the intestines of mice. However, the molecular mechanisms regulating *LEAP2* gene expression and secretion from the liver remain elusive. Further work, including the examination of liver-specific LEAP2 KO mice and measurements of hepatic arteriovenous LEAP2 differences, should address these missing links. In addition, it should be noted that the ChIP-Atlas currently does not contain much jejunal and duodenal-specific data. Therefore, the analysis of the putative LEAP2 enhancer-like signature from digestive tract is mostly based on colonic cancer samples and primary gastric samples.

To better understand the relationship between glucagon, insulin, ghrelin, and LEAP2, it is helpful to review the current evidence linking GHS-R1a signaling and LEAP2 to the pathophysiology of obesity and other metabolic diseases. Fasting plasma LEAP2 levels have been reported to positively correlate/associate with fasting plasma glucose and HbA1c levels, fasting serum insulin levels, and insulin resistance when assessed in individuals with prediabetes and obesity,[20] in people spanning several BMI categories,[15] and finally, in healthy individuals vs. people with type 2 diabetes[43] (for HbA1c only). Our studies suggest that neither blood glucose levels nor hepatic glucose availability affects LEAP2 regulation (an increase in these parameters did not affect LEAP2 regulation in mice, while an increase in blood glucose with high glucagon infusion[44] was associated with decreased plasma LEAP2). Accordingly, it could be speculated that the high insulin levels as opposed to high glucose levels are driving the increased circulating levels of LEAP2. In this case, the upregulation may occur through pathways that are less sensitive to the attenuated insulin signaling associated with insulin resistance (lipogenic vs. glucoregulatory pathways).[45]

LEAP2 levels are also reported to correlate with hepatic lipid content and to be increased in individuals and animal models with hepatic steatosis.[20,23] Analyzing two snRNA-seq datasets with best hepatocyte coverage from our integrated liver cell atlas, we found that LEAP2 expression in hepatocytes from individuals with liver cirrhosis occurring with the progression of MAFLD and MASH is significantly higher than hepatocytes from individuals with no such medical record. This finding suggests an effect of hepatic lipid accumulation on LEAP2 regulation.

Although hyperglucagonemia is observed in individuals with obesity and type 2 diabetes,[46,47] likely due to the associated increase in levels of hepatic lipids in many of these individuals,[48] no correlation has been reported between LEAP2 and glucagon levels in individuals with prediabetes and overweight/obesity.[20] Furthermore, our findings suggest that hepatic glucagon resistance, occurring after 2 weeks of hypercaloric dietary

intervention,[44] is not associated with a change in basal plasma LEAP2 levels. Thus, while our studies suggest that insulin and glucagon exert opposite actions on LEAP2 regulation, it remains to be described how elevated concentrations of these hormones and the associated tissue resistance affect LEAP2 regulation in individuals living with metabolic disease.

In conclusion, while plasma LEAP2 levels decrease during infusions with glucagon in humans, the action of insulin is required for Leap2 upregulation associated with the consumption of a mixed meal in mice. Investigation of the human liver-filtered ChIP-Atlas revealed that insulin and glucagon-regulated transcription factors bind to a *LEAP2* proximal enhancer-like signature, supporting a role for these hormones in regulating *LEAP2* gene expression. Our integrated analysis of hepatic scRNA-seq and snRNA-seq data indicates that human hepatocytes are the primary contributors to hepatic LEAP2 expression. However, *in vitro* hepatocyte experiments failed to confirm the the regulation of LEAP2 by insulin and glucagon observed in mice and humans. Therefore, glucagon and insulin-dependent LEAP2 regulation appears to require inter-organ crosstalk, other cell types, and/or additional circulating factors. Thus, a complex interdependency of LEAP2, glucagon, and insulin actions might exist, influenced by temporal relationships and metabolic states. This underscores the need for further research in the endocrine and physiological regulation of LEAP2.

Limitations of the study

A limitation of the current study is the translation of the *in vivo* and *in vitro* experiments to a human setting. While our human experiments support that an endocrine interplay between glucagon and LEAP2 exists, it remains to be established whether our findings, suggesting that the action of insulin is needed for postprandial LEAP2 upregulation in mice, translate to humans. Finally, a validation of the role of insulin signaling in regulating postprandial LEAP2 levels in human volunteers is crucial to decipher if our findings are replicated in humans.

RESOURCE AVAILABILITY

Lead contact

Further information and requests for resources and reagents should be directed to and will be fulfilled upon reasonable request by the lead contact, Christoffer Clemmensen (chc@sund.ku.dk).

Materials availability

This study did not generate new unique reagents.

Data and code availability

- The data that support the findings of this study are contained within this manuscript, and the bulk RNA sequencing dataset is uploaded to GEO under accession number GSE287171. Also, raw sequencing files are available as Tables S1 and S2. Raw bioinformatics data in bed files are available from the UCSC Genome Browser and from the ChIP-Atlas and GEO, as indicated in the deposited data section of the key resources table.
- No custom code is generated. All data analysis, including the single-cell data analysis, was performed using public and peer-reviewed software tools, which were cited in the methods section of this manuscript.
- Any additional information required to reanalyze the data reported in this work paper is available from the lead contact upon request.

ACKNOWLEDGMENTS

The authors would like to acknowledge Rikke Sørensen, Jesper Damgaard, Lene Winther Takla, Jeanette de Wett Brodersen, Sebastién, Helle Iversen, and Rose Bøge Kildetoft (Global Drug Discovery, Novo Nordisk A/S, Måløv, Denmark) for technical laboratory support and Magnus Harder for statistical advice (Discovery and Development PKPD, Novo Nordisk A/S, Måløv, Denmark). V.B.I.J. was supported by a Peter & Emma Thomsen Scholarship during parts of the investigatory process of the project. A.K.J.G. was funded by the LifePharm Centre for In Vivo Pharmacology and the Department of Biomedical Sciences. C.C. was supported by a research grant the Novo Nordisk Foundation (grant number NNF22OC0073778). The Novo Nordisk Foundation Center for Basic Metabolic Research is an independent research center, based at the University of Copenhagen, Denmark, and partially funded by an unconditional donation from the Novo Nordisk Foundation (www.cbmr.ku.dk) (grant numbers NNF18CC0034900 and NNF23SA0084103).

AUTHOR CONTRIBUTIONS

Conceptualization, V.B.I.J., M.M., N.P., D.D., and A.K.J.G.; methodology, V.B.I.J., M.M., N.P., D.D., M.P.S., M.F.G.G., A.B.L., F.K.K., C.A.P.-M., and A.K.J.G.; software, V.B.I.J. and C.A.P.-M.; validation, all authors; formal analysis, V.B.I.J., C.A.P.-M., and A.K.J.G.; investigation, V.B.I.J., M.M., N.P., D.D., M.P.S., M.F.G.G., A.B.L., F.K.K., C.A.P.-M., and A.K.J.G.; resources, M.M., N.P., D.D., F.K.K., J.L., B.H., and C.C.; data curation, V.B.I.J., M.P.S., C.A.P.-M., and A.K.J.G.; writing – original draft preparation, V.B.I.J.; writing – review and editing, V.B.I.J., F.K.K., M.P.S., M.M., N.P., J.L., B.H., B.K.M., W.F.J.H., N.P., C.C., and A.K.J.G.; supervision, M.M., N.P., C.C., and A.K.J.G.; project administration, V.B.I.J. and A.K.J.G.; funding acquisition, M.M., N.P., D.D., F.K.K., J.L., C.C., and B.H. All authors have read and agreed to the published version of the manuscript.

DECLARATION OF INTERESTS

M.M., N.P., D.D., B.K.M., F.K.K., C.A.P.-M., and W.F.J.H. are employed at Novo Nordisk. A.B.L. has received research support from Novo Nordisk and honoraria as a speaker for Boehringer Ingelheim, Novo Nordisk, and AstraZeneca. C.C. is a co-founder of Ousia Pharma. A.K.J.G. is employed at Zealand Pharma.

STAR★METHODS

Detailed methods are provided in the online version of this paper and include the following:

- KEY RESOURCES TABLE
- EXPERIMENTAL MODEL AND STUDY PARTICIPANT DETAILS
  - Human participants
  - Animals
  - Cell lines
  - Primary cell cultures
- METHOD DETAILS
  - Human studies
  - Mouse studies
  - Primary cell cultures
  - Cell lines
  - Bioinformatics
- QUANTIFICATION AND STATISTICAL ANALYSIS
- ADDITIONAL RESOURCES
  - Clinical trial registries and links

SUPPLEMENTAL INFORMATION

Supplemental information can be found online at https://doi.org/10.1016/j.xcrm.2025.101996.

CellPress
OPEN ACCESS

Received: February 12, 2024
Revised: September 14, 2024
Accepted: February 10, 2025
Published: March 6, 2025

REFERENCES

1. Mani, B.K., and Zigman, J.M. (2017). Ghrelin as a Survival Hormone. Trends Endocrinol. Metabol. *28*, 843–854.
2. Andrews, Z.B. (2019). The next big LEAP2 understanding ghrelin function. J. Clin. Investig. *129*, 3542–3544.
3. Zhao, T.-J., Liang, G., Li, R.L., Xie, X., Sleeman, M.W., Murphy, A.J., Valenzuela, D.M., Yancopoulos, G.D., Goldstein, J.L., and Brown, M.S. (2010). Ghrelin O-acyltransferase (GOAT) is essential for growth hormone-mediated survival of calorie-restricted mice. Proc. Natl. Acad. Sci. USA *107*, 7467–7472.
4. Zigman, J.M., Bouret, S.G., and Andrews, Z.B. (2016). Obesity Impairs the Action of the Neuroendocrine Ghrelin System. Trends Endocrinol. Metabol. *27*, 54–63.
5. Briggs, D.I., and Andrews, Z.B. (2011). Metabolic status regulates ghrelin function on energy homeostasis. Neuroendocrinology *93*, 48–57.
6. Kojima, M., Hosoda, H., Date, Y., Nakazato, M., Matsuo, H., and Kangawa, K. (1999). Ghrelin is a growth-hormone-releasing acylated peptide from stomach. Nature *402*, 656–660.
7. Nakazato, M., Murakami, N., Date, Y., Kojima, M., Matsuo, H., Kangawa, K., and Matsukura, S. (2001). A role for ghrelin in the central regulation of feeding. Nature *409*, 194–198.
8. Tschöp, M., Smiley, D.L., and Heiman, M.L. (2000). Ghrelin induces adiposity in rodents. Nature *407*, 908–913.
9. Mani, B.K., Shankar, K., and Zigman, J.M. (2019). Ghrelin's Relationship to Blood Glucose. Endocrinology *160*, 1247–1261.
10. Ge, X., Yang, H., Bednarek, M.A., Galon-Tilleman, H., Chen, P., Chen, M., Lichtman, J.S., Wang, Y., Dalmas, O., Yin, Y., et al. (2018). LEAP2 Is an Endogenous Antagonist of the Ghrelin Receptor. Cell Metab. *27*, 461–469.e6.
11. M'Kadmi, C., Cabral, A., Barrile, F., Giribaldi, J., Cantel, S., Damian, M., Mary, S., Denoyelle, S., Dutertre, S., Péraldi-Roux, S., et al. (2019). N-Terminal Liver-Expressed Antimicrobial Peptide 2 (LEAP2) Region Exhibits Inverse Agonist Activity toward the Ghrelin Receptor. J. Med. Chem. *62*, 965–973.
12. Wang, J.-H., Li, H.Z., Shao, X.X., Nie, W.H., Liu, Y.L., Xu, Z.G., and Guo, Z.Y. (2019). Identifying the binding mechanism of LEAP2 to receptor GHSR1a. FEBS J. *286*, 1332–1345.
13. Li, H.-Z., Shou, L.L., Shao, X.X., Liu, Y.L., Xu, Z.G., and Guo, Z.Y. (2020). Identifying key residues and key interactions for the binding of LEAP2 to receptor GHSR1a. Biochem. J. *477*, 3199–3217.
14. Holst, B., Holliday, N.D., Bach, A., Elling, C.E., Cox, H.M., and Schwartz, T.W. (2004). Common Structural Basis for Constitutive Activity of the Ghrelin Receptor Family. J. Biol. Chem. *279*, 53806–53817.
15. Mani, B.K., Puzziferri, N., He, Z., Rodriguez, J.A., Osborne-Lawrence, S., Metzger, N.P., Chhina, N., Gaylinn, B., Thorner, M.O., Thomas, E.L., et al. (2019). LEAP2 changes with body mass and food intake in humans and mice. J. Clin. Investig. *129*, 3909–3923.
16. Barrile, F., M'Kadmi, C., De Francesco, P.N., Cabral, A., García Romero, G., Mustafá, E.R., Cantel, S., Damian, M., Mary, S., Denoyelle, S., et al. (2019). Development of a novel fluorescent ligand of growth hormone secretagogue receptor based on the N-Terminal Leap2 region. Mol. Cell. Endocrinol. *498*, 110573.
17. Islam, M.N., Mita, Y., Maruyama, K., Tanida, R., Zhang, W., Sakoda, H., and Nakazato, M. (2020). Liver-expressed antimicrobial peptide 2 antagonizes the effect of ghrelin in rodents. J. Endocrinol. *244*, 13–23.
18. Hagemann, C.A., Jensen, M.S., Holm, S., Gasbjerg, L.S., Byberg, S., Skov-Jeppesen, K., Hartmann, B., Holst, J.J., Dela, F., Vilsbøll, T., et al. (2022). LEAP2 reduces postprandial glucose excursions and ad libitum food intake in healthy men. Cell Rep. Med. *3*, 100582.
19. ENGLUND, A., HAGEMANN, C.A., GASBJERG, L.S., and KNOP, F.K. (2023). 285-LB: LEAP2 Reduces Preprandial and Postprandial Glucose Levels and Ad Libitum Food Intake in Obese Men. Diabetes *72*, 285–LB.
20. Byberg, S., Blond, M.B., Holm, S., Amadid, H., Nielsen, L.B., Clemmensen, K.K.B., Færch, K., and Holst, B. (2023). LEAP2 is Associated with Cardiometabolic Markers, but is Unchanged by Antidiabetic Treatment in People with Prediabetes. Am. J. Physiol. Endocrinol. Metab. *325*, E244–E251. https://doi.org/10.1152/ajpendo.00023.2023.
21. Holm, S., Husted, A.S., Skov, L.J., Morville, T.H., Hagemann, C.A., Jorsal, T., Dall, M., Jakobsen, A., Klein, A.B., Treebak, J.T., et al. (2022). Beta-Hydroxybutyrate Suppresses Hepatic Production of the Ghrelin Receptor Antagonist LEAP2. Endocrinology *163*, bqac038.
22. Bhargava, R., Luur, S., Rodriguez Flores, M., Emini, M., Prechtl, C.G., and Goldstone, A.P. (2023). Postprandial Increases in Liver-Gut Hormone LEAP2 Correlate with Attenuated Eating Behavior in Adults Without Obesity. J. Endocr. Soc. *7*, bvad061.
23. Ma, X., Xue, X., Zhang, J., Liang, S., Xu, C., Wang, Y., and Zhu, J. (2021). Liver Expressed Antimicrobial Peptide 2 is Associated with Steatosis in Mice and Humans. Exp. Clin. Endocrinol. Diabetes *129*, 601–610.
24. Lu, X., Huang, L., Huang, Z., Feng, D., Clark, R.J., and Chen, C. (2021). LEAP-2: An Emerging Endogenous Ghrelin Receptor Antagonist in the Pathophysiology of Obesity. Front. Endocrinol. *12*, 717544.
25. Berryman, D.E., Glad, C.A.M., List, E.O., and Johannsson, G. (2013). The GH/IGF-1 axis in obesity: pathophysiology and therapeutic considerations. Nat. Rev. Endocrinol. *9*, 346–356.
26. Gradel, A.K.J., Holm, S.K., Byberg, S., Merkestein, M., Hogendorf, W.F.J., Lund, M.L., Buijink, J.A., Damgaard, J., Lykkesfeldt, J., and Holst, B. (2023). The dietary regulation of LEAP2 depends on meal composition in mice. FASEB J. *37*, e22923.
27. Shankar, K., Takemi, S., Gupta, D., Varshney, S., Mani, B.K., Osborne-Lawrence, S., Metzger, N.P., Richard, C.P., Berglund, E.D., and Zigman, J.M. (2021). Ghrelin cell-expressed insulin receptors mediate meal- and obesity-induced declines in plasma ghrelin. JCI Insight *6*, e146983.
28. Gagnon, J., and Anini, Y. (2013). Glucagon stimulates ghrelin secretion through the activation of MAPK and EPAC and potentiates the effect of norepinephrine. Endocrinology *154*, 666–674.
29. Chabot, F., Caron, A., Laplante, M., and St-Pierre, D.H. (2014). Interrelationships between ghrelin, insulin and glucose homeostasis: Physiological relevance. World J. Diabetes *5*, 328–341.
30. Tschöp, M., Weyer, C., Tataranni, P.A., Devanarayan, V., Ravussin, E., and Heiman, M.L. (2001). Circulating ghrelin levels are decreased in human obesity. Diabetes *50*, 707–709.
31. McCowen, K.C., Maykel, J.A., Bistrian, B.R., and Ling, P.R. (2002). Circulating ghrelin concentrations are lowered by intravenous glucose or hyperinsulinemic euglycemic conditions in rodents. J. Endocrinol. *175*, R7–R11.
32. Caixás, A., Bashore, C., Nash, W., Pi-Sunyer, F., and Laferrère, B.I. (2002). unlike food intake, does not suppress ghrelin in human subjects. J. Clin. Endocrinol. Metab. *87*, 1902.
33. Broglio, F., Gottero, C., Prodam, F., Destefanis, S., Gauna, C., Me, E., Riganti, F., Vivenza, D., Rapa, A., Martina, V., et al. (2004). Ghrelin secretion is inhibited by glucose load and insulin-induced hypoglycaemia but unaffected by glucagon and arginine in humans. Clin. Endocrinol. *61*, 503–509.
34. Al-Massadi, O., Müller, T., Tschöp, M., Diéguez, C., and Nogueiras, R. (2018). Ghrelin and LEAP-2: Rivals in Energy Metabolism. Trends Pharmacol. Sci. *39*, 685–694.
35. Bayle, M., Péraldi-Roux, S., Gautheron, G., Cros, G., Oiry, C., and Neasta, J. (2022). Liver-Expressed Antimicrobial Peptide 2 antagonizes the insulinostatic effect of ghrelin in rat isolated pancreatic islets. Fundam. Clin. Pharmacol. *36*, 375–377.
36. Hagemann, C.A., Zhang, C., Hansen, H.H., Jorsal, T., Rigbolt, K.T.G., Madsen, M.R., Bergmann, N.C., Heimbürger, S.M.N., Falkenhahn, M.,

Theis, S., et al. (2021). Identification and Metabolic Profiling of a Novel Human Gut-derived LEAP2 Fragment. J. Clin. Endocrinol. Metab. *106*, e966–e981.

37. Ribeiro, I.M.R., and Antunes, V.R. (2018). The role of insulin at brain-liver axis in the control of glucose production. Am. J. Physiol. Gastrointest. Liver Physiol. *315*, G538–G543.
38. Plum, L., Belgardt, B.F., and Brüning, J.C. (2006). Central insulin action in energy and glucose homeostasis. J. Clin. Investig. *116*, 1761–1766.
39. Ribeiro, I.M.R., Ferreira-Neto, H.C., and Antunes, V.R. (2015). Subdiaphragmatic vagus nerve activity and hepatic venous glucose are differentially regulated by the central actions of insulin in Wistar and SHR. Phys. Rep. *3*, e12381.
40. Girard, J. (2006). Insulin's effect on the liver: "Direct or indirect?" continues to be the question. J. Clin. Investig. *116*, 302–304.
41. Edgerton, D.S., Kraft, G., Smith, M., Farmer, B., Williams, P.E., Coate, K.C., Printz, R.L., O'Brien, R.M., and Cherrington, A.D. (2017). Insulin's direct hepatic effect explains the inhibition of glucose production caused by insulin secretion. JCI Insight *2*, e91863.
42. Edgerton, D.S., Lautz, M., Scott, M., Everett, C.A., Stettler, K.M., Neal, D.W., Chu, C.A., and Cherrington, A.D. (2006). Insulin's direct effects on the liver dominate the control of hepatic glucose production. J. Clin. Investig. *116*, 521–527.
43. Li, J., Huang, P., Xiong, J., Liang, X., Li, M., Ke, H., Chen, C., Han, Y., Huang, Y., Zhou, Y., et al. (2022). Serum levels of ghrelin and LEAP2 in patients with type 2 diabetes mellitus: correlation with circulating glucose and lipids. Endocr. Connect. *11*, e220012.
44. Suppli, M.P., Høgedal, A., Bagger, J.I., Chabanova, E., van Hall, G., Forman, J.L., Christensen, M.B., Albrechtsen, N.J.W., Holst, J.J., and Knop, F.K. (2024). Signs of Glucagon Resistance After a 2-Week Hypercaloric Diet Intervention. J. Clin. Endocrinol. Metab. *109*, 955–967. https://doi.org/10.1210/clinem/dgad666.
45. Otero, Y.F., Stafford, J.M., and McGuinness, O.P. (2014). Pathway-selective insulin resistance and metabolic disease: the importance of nutrient flux. J. Biol. Chem. *289*, 20462–20469.
46. Knop, F.K., Vilsbøll, T., Madsbad, S., Holst, J.J., and Krarup, T. (2007). Inappropriate suppression of glucagon during OGTT but not during isoglycaemic i.v. glucose infusion contributes to the reduced incretin effect in type 2 diabetes mellitus. Diabetologia *50*, 797–805.
47. Ranson, J.H. (1989). Endoscopy for gallstone pancreatitis. Gastroenterology *97*, 1592–1593.
48. Junker, A.E., Gluud, L., Holst, J.J., Knop, F.K., and Vilsbøll, T. (2016). Diabetic and nondiabetic patients with nonalcoholic fatty liver disease have an impaired incretin effect and fasting hyperglucagonaemia. J. Intern. Med. *279*, 485–493.
49. Patro, R., Duggal, G., Love, M.I., Irizarry, R.A., and Kingsford, C. (2017). Salmon provides fast and bias-aware quantification of transcript expression. Nat. Methods *14*, 417–419.
50. Love, M.I., Huber, W., and Anders, S. (2014). Moderated estimation of fold change and dispersion for RNA-seq data with DESeq2. Genome Biol. *15*, 550.
51. Grøndahl, M.F., Lund, A.B., Bagger, J.I., Petersen, T.S., Wewer Albrechtsen, N.J., Holst, J.J., Vilsbøll, T., Christensen, M.B., and Knop, F.K. (2021). Glucagon Clearance Is Preserved in Type 2 Diabetes. Diabetes *71*, 73–82.
52. Petersen, N., Reimann, F., Bartfeld, S., Farin, H.F., Ringnalda, F.C., Vries, R.G.J., van den Brink, S., Clevers, H., Gribble, F.M., and de Koning, E.J.P. (2014). Generation of L cells in mouse and human small intestine organoids. Diabetes *63*, 410–420.
53. Sato, T., Vries, R.G., Snippert, H.J., van de Wetering, M., Barker, N., Stange, D.E., van Es, J.H., Abo, A., Kujala, P., Peters, P.J., and Clevers, H. (2009). Single Lgr5 stem cells build crypt-villus structures in vitro without a mesenchymal niche. Nature *459*, 262–265.
54. Snippert, H.J., van der Flier, L.G., Sato, T., van Es, J.H., van den Born, M., Kroon-Veenboer, C., Barker, N., Klein, A.M., van Rheenen, J., Simons, B.D., and Clevers, H. (2010). Intestinal crypt homeostasis results from neutral competition between symmetrically dividing Lgr5 stem cells. Cell *143*, 134–144.
55. Sato, T., Stange, D.E., Ferrante, M., Vries, R.G.J., Van Es, J.H., Van den Brink, S., Van Houdt, W.J., Pronk, A., Van Gorp, J., Siersema, P.D., and Clevers, H. (2011). Long-term expansion of epithelial organoids from human colon, adenoma, adenocarcinoma, and Barrett's epithelium. Gastroenterology *141*, 1762–1772.
56. Hare, K.J., Vilsbøll, T., Asmar, M., Deacon, C.F., Knop, F.K., and Holst, J.J. (2010). The glucagonostatic and insulinotropic effects of glucagon-like peptide 1 contribute equally to its glucose-lowering action. Diabetes *59*, 1765–1770.
57. Boden, G., Tappy, L., Jadali, F., Hoeldtke, R.D., Rezvani, I., and Owen, O.E. (1990). Role of glucagon in disposal of an amino acid load. Am. J. Physiol. *259*, E225–E232.
58. Polański, K., Young, M.D., Miao, Z., Meyer, K.B., Teichmann, S.A., and Park, J.E. (2020). BBKNN: fast batch alignment of single cell transcriptomes. Bioinformatics *36*, 964–965.
59. Wolf, F.A., Angerer, P., and Theis, F.J. (2018). SCANPY: large-scale single-cell gene expression data analysis. Genome Biol. *19*, 15.
60. Melé, M., Ferreira, P.G., Reverter, F., DeLuca, D.S., Monlong, J., Sammeth, M., Young, T.R., Goldmann, J.M., Pervouchine, D.D., Sullivan, T.J., et al. (2015). The human transcriptome across tissues and individuals. Science *348*, 660–665.
61. Carithers, L.J., Ardlie, K., Barcus, M., Branton, P.A., Britton, A., Buia, S.A., Compton, C.C., DeLuca, D.S., Peter-Demchok, J., Gelfand, E.T., et al. (2015). A Novel Approach to High-Quality Postmortem Tissue Procurement: The GTEx Project. Biopreserv. Biobanking *13*, 311–319.
62. Lonsdale, J., Thomas, J., Salvatore, M., Phillips, R., Lo, E., Shad, S., Hasz, R., Walters, G., Garcia, F., Young, N., et al. (2013). The Genotype-Tissue Expression (GTEx) project. Nat. Genet. *45*, 580–585.
63. Oki, S., Ohta, T., Shioi, G., Hatanaka, H., Ogasawara, O., Okuda, Y., Kawaji, H., Nakaki, R., Sese, J., and Meno, C. (2018). ChIP-Atlas: a data-mining suite powered by full integration of public ChIP-seq data. EMBO Rep. *19*, e46255.
64. Zou, Z., Ohta, T., Miura, F., and Oki, S. (2022). ChIP-Atlas 2021 update: a data-mining suite for exploring epigenomic landscapes by fully integrating ChIP-seq, ATAC-seq and Bisulfite-seq data. Nucleic Acids Res. *50*, W175–W182.
65. Cheng, X., Kim, S.Y., Okamoto, H., Xin, Y., Yancopoulos, G.D., Murphy, A.J., and Gromada, J. (2018). Glucagon contributes to liver zonation. Proc. Natl. Acad. Sci. USA *115*, E4111–E4119.

STAR★METHODS

KEY RESOURCES TABLE

REAGENT or RESOURCE	SOURCE	IDENTIFIER
Chemicals, peptides, and recombinant proteins		
S961	Novo Nordisk	NNC0069-0961
Insulin	Novo Nordisk	NNC0121-0308
Insulin	Novo Nordisk	Actrapid
Casein	Sigma Aldrich	Cas. no. 9000-71-9
Complete IntestiCult™ Organoid Growth Medium (Mouse)	Stemcell Technologies	Cat. No. #06005
Mouse RSPO	Biotechne	Cat. No. #3474-RS
Mouse Noggin	Biotechne	Cat. No. #6997-NG
Mouse EGF	Biotechne	Cat. No. #2028-EG
Dexamethasone	Sigma Aldrich	Cat. No. #D1159
Critical commercial assays		
LEAP2 ELISA kit	Phoenix Pharmaceuticals Inc	Cat. No. EK-075-40
AlphaScreen, SureFire, Akt 1/2/3 p-S473 Assay Kit	PerkinElmer	Cat. No. TGRA4S10k
RNeasy Mini Kit	Qiagen	Cat. No. 74104
iScript™ cNDA Synthesis Kit	Bio-rad Laboratories	Cat. No. M87EWZESH
NEBNext® Ultra™ II Directional RNA Library Prep Kit for Illumina®	New England BioLabs	NEB #E7765
Deposited data		
Bulk RNA sequencing	NCBI Gene Expression Omnibus	GSE287171 https://www.ncbi.nlm.nih.gov/geo/query/acc.cgi?acc=GSE287171
Single cell RNA sequencing	NCBI Gene Expression Omnibus	GSE136103 https://www.ncbi.nlm.nih.gov/geo/query/acc.cgi?acc=GSE136103
Single cell RNA sequencing	NCBI Gene Expression Omnibus	GSE185477 https://www.ncbi.nlm.nih.gov/geo/query/acc.cgi?acc=GSE185477
Single nucleus RNA sequencing	NCBI Gene Expression Omnibus	GSE189175 https://www.ncbi.nlm.nih.gov/geo/query/acc.cgi?acc=GSE189175
Single nucleus RNA sequencing	NCBI Gene Expression Omnibus	GSE189600 https://www.ncbi.nlm.nih.gov/geo/query/acc.cgi?acc=GSE189600
Single nucleus RNA sequencing	NCBI Gene Expression Omnibus	GSE192740 https://www.ncbi.nlm.nih.gov/geo/query/acc.cgi?acc=GSE192740
Single nucleus RNA sequencing	NCBI Gene Expression Omnibus	GSE212837 https://www.ncbi.nlm.nih.gov/geo/query/acc.cgi?acc=GSE212837
Bulk RNA sequencing	NCBI Gene Expression Omnibus	GSE110673 https://www.ncbi.nlm.nih.gov/geo/query/acc.cgi?acc=GSE110673
Human reference genome NCBI build 37, GRCh37	Genome Reference Consortium	http://www.ncbi.nlm.nih.gov/projects/genome/assembly/grc/human/
Human reference genome NCBI build 38, GRCh38/hg38	Genome Reference Consortium	http://www.ncbi.nlm.nih.gov/projects/genome/assembly/grc/human/
NIH Genotype-Tissue Expression (GTEx) project	GTEx LDACC at The Broad Institute of MIT and Harvard	Release V8 dbGaP Accession phs000424.v8.p2
ChIP-Atlas	NIG Supercomputer system and JST NBDC JPMJND2202	https://chip-atlas.org/
Experimental models: Cell lines		
Primary hepatocytes	Gibco	#MSCP10 LOT#MC959
Mouse jejunal organoids	C57BL/6J mouse	Derived from C57BL/6J mouse jejunum
HepG2-IGFR-KO cells	Novo Nordisk	NA

(*Continued on next page*)

Continued

REAGENT or RESOURCE	SOURCE	IDENTIFIER
Experimental models: Organisms/strains		
Mouse: C57BL/6J	Charles River	Strain Code: 027
Oligonucleotides		
Primers for RT-qPCR, see Tables S1 and S2	TaqMan from ThermoFischer and this paper	See Tables S1 and S2
Software and algorithms		
R statistical software	R Core Team	https://www.R-project.org/
GraphPad Prism 10	GraphPad	https://www.graphpad.com/
Microsoft Excel	Microsoft Corporation	https://www.microsoft.com/en-us/microsoft-365/excel
Integrative Genomics Viewer	UC San Diego and the Broad Institute	https://igv.org/
Quantstudio 12K flex	Thermo Fisher	NA
Salmon	Patro et al.[49]	https://combine-lab.github.io/salmon/
DEseq2	Love et al.[50]	https://bioconductor.org/packages/devel/bioc/vignettes/DESeq2/inst/doc/DESeq2.html
BBKNN	Polánski et al.[58]	https://github.com/Teichlab/bbknn
Scanpy	Wolf et al.[59]	v1.9.3

EXPERIMENTAL MODEL AND STUDY PARTICIPANT DETAILS

Human participants

Human plasma samples were obtained from 20 healthy individuals undergoing pancreatic somatostatin clamps or from 32 individuals with or without type 2 diabetes and/or diabetes receiving glucagon infusions. In both cases, the studies were approved by the Scientific-Ethical Committee of the Capital Region of Denmark (registration no. H-20036246 and H-1-2014-066) and registered as clinical trials (ID: NCT04859322 and ID: NCT02475421). The studies were performed in accordance with the principles of the 7th Revision of the Declaration of Helsinki. Informed consent was obtained from all participants. For the study of healthy volunteers, participants were between 20 and 65 years of age and all had a normal dietary pattern in accordance with the Nordic Nutrition Recommendations. All participants were males, limiting any gender-specific analyses. Whether the results obtained pertain to females should be addressed in future investigations. The absence of an analysis of the influence of gender limits the study's generalization. For the study of individuals with or without type 2 diabetes and/or diabetes, the type 2 diabetes group contained 8 lean individuals (5 males and 3 females) and 8 individuals with obesity (4 males and 4 females). In the group without type 2 diabetes, the same gender and BMI proportions were matched to that of the type 2 diabetes group. In this study the average age in years was 60.1 for lean individuals with type 2 diabetes and 57.8 for individuals with obesity and type 2 diabetes. In the group without type 2 diabetes, the average age was 62.1 years for those that were lean and 55.5 for those that were obese. There was no significant difference between these parameters. Given the rather limited sample size, there was no power to observe any gender-specific association of the LEAP2 levels over time from the beginning of the glucagon infusion. This limits the study's generalization. The duration of type 2 diabetes in years among individuals with and without obesity were not significant different. Details pertaining to the experimental setups involving human participants can be found in "method details". For the human dietary intervention study and pancreatic somatostatin clamp, human plasma samples were obtained from 20 healthy individuals undergoing pancreatic somatostatin clamps at three experimental days. The primary outcomes of this trial, from which the plasma samples were obtained, have been reported in accordance with ICJME previously.[44] The study was approved by the Research Ethics Committee of the Capital Region of Denmark (reg.no. H-20036246), registered with Clinicaltrials.gov (ID: NCT04859322), and was conducted in accordance with the latest revision of the Declaration of Helsinki. For detailed characteristics of participants and experimental designs, we refer to Suppli et al.[44] For glucagon infusions in human patients, individuals with type 2 diabetes and/or obesity and matched healthy controls were recruited, and the primary outcomes of this trial, from which the plasma samples were obtained, and details on experimental design, screening, and study participants, have been reported in accordance with ICJME previously.[51] After screening, individuals underwent a single identical experimental day. At the experimental day, participants were studied while resting in a bed following an overnight fast (for details please refer to Grøndahl et al. 2021[51]). Participants had two cannulas inserted into their cubital veins; one for infusion of glucagon, one for collection of blood.

Animals

Experiments and procedures in animal models were approved by the Danish Animal Experiment Inspectorate (Licence no. 2019-15-0201-00206 and license no. 2023-15-0201-01442). To investigate the role of insulin in the LEAP2 upregulation associated with

consumption of a meal, the effect of insulin receptor antagonism on the LEAP2 response associated with a mixed meal was assessed in 12-week-old male C57BL/6J mice. The same strain was used for the casein study and for acute insulin treatment in diet-induced obese mice as well as for the glucagon analogue treatment. For experimental work with mice, only male mice were used. Therefore, no statement about the influence of sex on the obtained results is available. This limits the study's generalization.

Cell lines

The only cell line used in this study was HepG2-IGF1R-KO cells and where bulk RNA-seq was performed. Briefly, HepG2-IGF1R-KO cells were cultured and maintained in DMEM supplemented with 10% FBS. Medium was aspirated and replaced with fresh medium every 2–3 days. Cells were split 1:4 every 3 days by aspiration of medium, washing once with PBS and trypsinization (0.25% Trypsin-EDTA solution, #T4049, Sigma).

Primary cell cultures

Primary cell cultures used in this manuscript include mouse primary hepatocytes (Gibco Cryo Mouse Hepatocytes) (#MSCP10 LOT#MC959, Thermo Fischer Scientific, Frederick MD, USA), human intestinal organoids purchased from Hub Organoid Technology (HUB, Utrecht, Netherlands, cataloged at huborganoids.nl), and mouse intestinal crypts that were isolated from C57BL/6J mouse jejunum, as described previously[52–55] and were seeded into Matrigel (BD Biosciences), in which they grew into organoids.[53,55]

METHOD DETAILS

Human studies

Twenty healthy male individuals with normal dietary patterns were recruited and examined on three identical experimental days (Figure 1A): at baseline (Day A), after a two-week hypercaloric diet intervention (Day B) and after an eight-week recovery period after the intervention period (Day C). The dietary intervention included an average intake of 4,641 kcal/day for two weeks and participants were asked to maintain a sedentary lifestyle. The original dietary intervention protocol is included in Suppli et al.[44] The participants were recruited from February 2021. At the day of the experiments, after a 10 h overnight fast, cannulas were inserted in both cubital veins: one for blood sampling and one for administering infusions. A stable [6,6-$^2H_2$]-glucose isotope was infused at time −120 min (prime: 26.4 μmol × kg^{-1}; continuous infusion: 0.6 μmol × kg^{-1} × min^{-1}). After 2 h of infusion (when tracer steady-state had been achieved), the individual underwent 3-h pancreatic clamps with somatostatin (450 μg × h^{-1}) to inhibit the endocrine pancreas. At the same time (time 0 min), infusions of insulin (0.1 mU × kg^{-1} × min^{-1}) and glucagon (0.6 ng × kg^{-1} × min^{-1}) were initiated to maintain basal systemic plasma concentrations of the two hormones in accordance with previous studies.[56] At time 60 min, the infusion rate of glucagon was increased to 4.0 ng × kg^{-1} × min^{-1}, producing high physiological plasma levels of glucagon.[57] To maintain tracer steady-state, an infusion of isotonic saline was adjusted to result in a constant total infusion rate of 200 mL × h^{-1}. For analyses of plasma LEAP2 levels at timepoints −15, 60, 120, and 180 min, blood was collected in chilled tubes containing EDTA, centrifuged at 1,200 *g* and 4°C and stored at −20°C until batch analysis.

For the glucagon infusions in human patients, at time point 0 min, a 60 min period of glucagon infusion was initiated (4 ng/kg/min = 1.15 pmol/kg/min). At the termination of the infusion period (at 60 min), a washout period of another 60 min began. With respect to glucagon analyses, blood was added to chilled tubes containing EDTA, aprotinin (500 kIU/mL blood, Trasylol; Bayer, Leverkusen, Germany), and a specific dipeptidylpeptidase 4 inhibitor (valine-pyrrolidine, final concentration 0.01 mmol/L; a gift from Novo Nordisk, Bagsværd, Denmark), and its change in pM calculated and reported following plasma isolation. For the analyses of C-peptide, blood was collected in plain tubes and left to coagulate (20 min at room temperature). All blood samples were centrifuged for 20 min at 1,200*g* and 4°C, and plasma was transferred to ice-chilled storage tubes. Plasma samples for glucagon analyses were stored at −20°C. Blood samples at −15 min, 60 min, and 120 min were analyzed for plasma LEAP2 levels as described below. The study was approved by the Scientific-Ethical Committee of the Capital Region of Denmark (registration no. H-1-2014-066) and registered as a clinical trial. The study was performed in accordance with the principles of the 7th Revision of the Declaration of Helsinki.

Mouse studies

All procedures performed in mice in this study have been approved by the Danish Animal Experiment Inspectorate (Licence no. 2019-15-0201-00206). Male C57BL/6J mice (Charles River, Germany) were single housed in cages enriched with bedding and nesting material, gnawing stick and shelter (two mice per cage with cage divider). The cages were kept at a constant temperature 22 ± 2°C and mice were exposed to a normal 12-h light/dark cycle (from 6:00 a.m.). Mice had free access to chow diet (Altromin #1324, Brogaarden, Lynge, Denmark) and water at all times unless otherwise specified. All mice were randomly allocated to the study groups by simple randomisation (Microsoft Excel, Microsoft Corporation, Washington, USA), thereby minimizing the effect of cage and treatment order on study outcome. Oral gavages of meal challenges were performed at 9:00 a.m. Male C57BL/6J mice aged 12 weeks were included to assess the effect of protein on the regulation of LEAP2. All mice were fasted for 16 h prior to oral gavage of casein (5% in water, 10 mL/kg body weight, Cas. no. 9000-71-9 from Sigma Aldrich, 2860 Soeborg, Denmark) or a dose-matched volume of water (n = 8 per group). Blood was collected from the sublingual vein (∼80 μL) and the tail vein (∼5 μL) just prior to oral gavage which was followed by blood sampling at 30 min (tail blood only), 1- and 2-h post dosing. For the insulin receptor antagonism study, all mice were fasted for 14 h prior to subcutaneous (s.c.) dosing with the insulin receptor antagonist, S961 (NNC0069-0961, 400 nmol/kg,

Novo Nordisk, 2760 Måløv, Denmark) (n = 8) or vehicle (10mM sodium phosphate, 140mM sodium chloride, 0.007% polysorbate 20, pH 7.4) (n = 16). This was followed by oral gavage 2 h later with either 10 mL/kg water (n = 8, mice s.c. dosed with vehicle) or a mixed meal (n = 16, 240 kcal/100 mL, carbohydrate [49 kcal%], protein [16 kcal%], fat [35 kcal%]; Nutricia Nutridrink, Allerød, Denmark). Half of the mice that received mixed meal had been dosed with S961 (n = 8) and the other half vehicle (n = 8). Blood was collected from the sublingual vein (~80 μL) and the tail vein (~5 μL) just prior to oral gavage which was followed by blood sampling at 30 min (tail blood only), 1- and 2-h post dosing. All mice were euthanized by cervical dislocation at the end of the experiments. Tissue biopsies were collected from the left lateral liver lobe, duodenum, and jejunum (1–4 cm and 10–16 cm distally to the pyloric sphincter, respectively) and immediately frozen in liquid nitrogen. The biopsies were stored at −80°C until analysis. To examine the impact of insulin administration on adult male DIO mice or lean mice fed chow diet, mice were administered either i.p. insulin (0.75 U/kg, 5 μL/g body weight) or isovolumic saline (vehicle) (n = 8 in each group). Remnants of food were removed from cages at the time of the injection. Blood glucose levels were measured using blood from the tail tip and a handheld glucometer (Abbott) at timepoint 0 (just before i.p. injection of insulin), 30, 60, and 120 min after i.p injection of insulin, whereas plasma LEAP2 levels were measured as described below. To examine if gene expression levels of *Leap2* was affected by a long-acting glucagon treatment, DIO mice were treated daily with long-acting glucagon (NNC9204-0043, Novo Nordisk A/S, Maaloev) (30 nmol/kg, 5 μL/g body weight) or a vehicle solution (5 μL/g body weight) for 14 days. At the end of the experiment, liver tissue was harvested, and RT-qPCR was performed as described below. An overview of these study designs is provided in Figures 2A, 3A, and S4.

Blood samples

Sublingual blood samples were collected in EDTA tubes with aprotinin (2.5 μL Trasylol, Nordic Group B.V., Hoofddorp, Netherlands) and centrifuged at 6000 g, 4°C for 5 min. Plasma was isolated from the EDTA tubes and stored at −80°C until plasma analyses of LEAP2, insulin and glucagon levels. In order to determine blood glucose levels, 5 μL tail blood was collected in heparinized coated glass capillary tubes and immediately suspended in buffer (250 μL of EKF system solution, EKF-diagnostics GmbH, Barleben, Germany). Samples were analyzed using the glucose oxidase method (BIOSEN S-line, EKF-diagnostics, Barleben, Germany).

Tissue and plasma biochemistry

Quantification of plasma insulin and glucagon was performed with luminescent oxygen channelling immunoassay technology at Novo Nordisk. Lowest level of quantification for glucagon and insulin was 4 and 35 pmol/L, respectively. Tissue samples were prepared by homogenizing the biopsies in a 0.15 M sodium acetate buffer (pH = 4.9) containing 0.75% Triton X-100 (Sigma-Aldrich, Soeborg, Denmark). Tissuelyser II and 5 mm stainless aluminum beads (Qiagen, Hilden Germany) were used to homogenize the liver samples. The samples were subsequently placed on a heating block (95 ± 5°C) for 2 min before being placed on ice. The cooled homogenate from each liver sample was split into two aliquots. Amyloglucosidase (Sigma-Aldrich, Cas no. 9032-08-0, 2860 Soeborg, Denmark) was added to one of the aliquots which was then placed on a heating block (50°C) for 2 h to facilitate the breakdown of glycogen to glucose. Both aliquots were subsequently centrifuged at 9000 g for 10 min and the supernatant was used to measure liver biochemistry. Hepatic levels of triglycerides, total cholesterol, fatty acids (FA), aspartate transaminase (ASAT), alanine transaminase (ALAT), glucose, and glycogen were determined using the Cobas Pro c503 instrument (Roche Diagnostics GmbH, Mannheim, Germany) according to manufacturer's instructions. Levels of glycogen were calculated by subtracting the free glucose from the total glucose concentration (measured in untreated and amyloglucosidase treated samples, respectively).

Quantitative reverse transcription PCR

RNA from tissue and mouse hepatocytes was isolated using the RNeasy Mini Kit according to manufacturer's instructions (Qiagen, Hilden, Germany). TissueLyser II and 5 mm stainless steel beads were used to disrupt and homogenize tissue samples, and DNase digestion was facilitated by the RNase-Free DNase set (Qiagen, Hilden, Germany). RNA from tissue and mouse hepatocytes was collected in 30 μL RNase free water where 1 μL was used to determine RNA concentration and purity (Nanodrop 8000 Spectrophotometer, Thermo Fisher Scientific, Massachusetts, USA; mean A260/280~2). cDNA was subsequently synthesized using iScript cNDA Synthesis Kit (Bio-rad Laboratories, California, USA). Fifteen μL RNA in RNase free water was mixed with 4 μL iScript Reaction Mix and 1 μL iScript Reverse Transcriptase, generating a total reaction volume of 20 μL for cDNA synthesis and amplification (C1000 Touch Thermal Cycler, Bio-Rad Laboratories, California, USA). One μg RNA was used for the cDNA synthesis, followed by 1:10 dilution of cDNA in MilliQ water prior to qPCR analysis. TaqMan primers for qPCR were purchased from Thermo Fisher (Thermo Fisher Scientific, Massachusetts, USA). For RT-qPCR, 5 μL cDNA mixed with 6 μL Taqman, 0.6 μL TaqMan assay and 0.4 μL MilliQ water were added in each well. The fluorescence signal was measured on the Quantstudio 12K flex (Thermo Fisher Scientific, Waltham, Massachusetts, USA) from which the threshold cycle (C_t) values were extracted from the associated software. No-template controls were checked for either missing C_t values or values >35. mRNA level was reported as the average C_t value from duplicates or triplicates. Levels were normalised to constitutively expressed *Ywhaz* and the relative mRNA content was calculated by the $2^{-\Delta\Delta CT}$ method in Microsoft Excel (Microsoft Corporation, Washington, USA). Invariant mRNA level of reference genes across the study groups was confirmed by statistical comparisons across the groups (as described in quantification and statistical analysis). For an overview of genes for RT-qPCR and the associated primers, please refer to Table S1. For revision purposes, additional experimental work was analyzed using SYBR Green RT-qPCR (Figures S3B and S10A). Here, RT-qPCR was performed on 5 μL cDNA mixed with 5.5 μL PrecisionPLUS OneSTEP RT-qPCR master mix (Primer Design, York, United Kingdom), and 0.11 μL of both forward and reverse primers (primers summarized in Table S2).

ELISA

LEAP2 in plasma was analyzed with an ELISA kit for human and mouse LEAP2 detection (Cat. No. EK-075-40, Phoenix Pharmaceuticals Inc, Burligame, USA). Mouse plasma samples were diluted 1:50, human plasma samples 1:20, whereas cell medium was used undiluted before being analyzed in accordance with the manufacturer's instructions.

Primary cell cultures

Mouse primary hepatocytes: Gibco Cryo Mouse Hepatocytes (#MSCP10 LOT#MC959, Thermo Fischer Scientific, Frederick MD, USA) were thawed in a 37°C water bath and transferred immediately to 10 mL seeding media comprising of basic media containing 1 nM insulin (NNC0121-0308 batch #047.ins.05.2) and 10% FBS. The basic media contained Medium 199 with phenolred, glutamax and 5.5 mM glucose (Gibco # 41150) supplemented with 1% penicillin/streptomycin (Gibco # 15140-114) and 4 mg/mL dexamethasone (sigma #D1159). The cells were pelleted for 3 min at 55 g, and the medium was aspirated. Subsequently, pelleted cells were resuspended in 10 mL seeding medium and counted, and viability and aggregation were determined. Approximately 250.000 hepatocytes per well were seeded into 24-well collagen coated plates (biocat #354649) for ELISA and qPCR analyses. Approximately 50.000 hepatocytes per well were seeded into 96-well collagen coated plates (biocat #354649, Corning) for Surefire assays. After 4-5h post seeding, the medium was changed to basic medium supplemented with 0.1% FBS and thus starved overnight prior to the experiment. At the day of the experiment, starvation medium was aspirated, and cells were exposed to 20 mM glucose, 3 nM human insulin, 30 nM S961, in combination or alone as indicated or 100 nM glucagon, as indicated, for 4 h in a humidified incubator at 37°C with 5% CO_2 in a background of DMEM low glucose supplemented with 0.1% HSA that served as the control. For termination of the experiment, cells were immediately put on ice where medium was collected for ELISA. Cells were washed 3 times with cold PBS, snap-frozen in liquid nitrogen prior to addition of 350 μL RLT lysis buffer (Qiagen) and stored in −80°C freezers until RNA extraction for qPCR was performed as described above. For assessing insulin sensitivity, the phosphorylation state of Akt in hepatocyte lysates was determined using the AlphaScreen, SureFire, Akt 1/2/3 p-S473 Assay Kit (Cat. No. TGRA4S10k, PerkinElmer) according to manufacturer's instructions. Briefly, cells were incubated with different concentrations of human insulin or S961 in combination with a fixed human insulin concentration of 10 nM as indicated and incubated for 15 min at 37°C in a humidified incubator with 5% CO_2. Cell medium was then immediately removed, and the plate was placed on ice where cells were washed 2 times with 100 μL ice-cold PBS prior to being snap-frozen in liquid nitrogen and stored at −80°C until analysis following the assay protocol. Acceptor and donor beads were from the Protein A general IgG detection kit (PerkinElmer, Cat. # 6760617M) and the 384 well plate used for the assay was the AlphaPlate-384 (PerkinElmer, cat. # 6008359).

Human intestinal organoids purchased from Hub Organoid Technology (HUB, Utrecht, Netherlands, cataloged at huborganoids.nl) were cultured in Advanced DMEM/F12 (AD-DF^{+++}) (Cat. No. 12634-010, Gibco, Thermo Fischer Scientific, Frederick MD, USA) supplemented with 1% penicillin/streptomycin (Cat. No. 15140-114, Gibco, Thermo Fischer Scientific, Frederick MD, USA), 1% GlutaMax (Cat. No. 35050-038, Gibco, Thermo Fischer Scientific, Frederick MD, USA), and 1% 1M HEPES (Cat. No. 15630-056, Gibco, Thermo Fischer Scientific, Frederick MD, USA). Following growth factors were added: 200 ng/mL recombinant noggin (Cat. No. 120-10C, Peprotech, Thermo Fischer Scientific, Frederick MD, USA), 1:200 B27 (Cat. No. 12587010, Lifetechnologies, Thermo Fischer Scientific, Frederick MD, USA), 1 mM g N-Acetyl cysteine (Cat. No. A9165-25G, Sigma-Aldrich, Missouri, USA), 100 ng/mL recombinant human EGF (Cat. No. AF-100-15, Peprotech, Thermo Fischer Scientific, Frederick MD, USA), 10 nM gastrin (Cat. No. G9145, Sigma-Aldrich, Missouri, USA), and 1 μM A83-01 (Cat. No. 2939, Biotechne, Tocris) (2X Intestinal organoid base medium, 2X IBM medium). Human organoids were expanded in 1X IBM medium containing 25 mL AD-DF^{+++} per 50 mL expansion medium, 0.5 nM NGS-Wnt (Cat. No. N001, Immunoprecise Antibodies), 250 ng/mL human Rspondin-3 (Cat. No. 3500-RS/CF, Biotechne), 10 mM nicotinamide (Cat. No. N0636-100g, Sigma-Aldrich, Missouri, USA), 10 μM p38 inhibitor (Cat. No. S7067, Sigma-Aldrich, Missouri, USA), 50 μg/mL primocin (Cat. No. ant-PM-1, InvivoGen) and 10 μM ROCK inhibitor (Cat. No. Y-27632, dihydrochloride, Tocris 1254, Biotechne). Organoids were kept at 37°C in a humidified incubator with 5% CO_2 in an LDPE bag, and medium was refreshed every 2–3 days. Human duodenal HUB organoids were differentiated for 5 days in 1X IBM medium with 9.84 mL AD-DF^{+++} per 20mL combination differentiation medium, 0.1 nM NGS-Wnt, 250 ng/mL human Rspondin-3, 10 μM DAPT (Cat. No. D5942-25MG, Sigma-Aldrich, Missouri, USA) and 100 nM PD0325901 (Cat. No. PZ0162-25mg, Sigma-Aldrich, Missouri, USA) prior to the experiment. On the day of the experiments, human intestinal organoids were partially starved for 4h in Dulbecco's Modified Eagle's Medium (DMEM) – low glucose (Cat. No. D2429, Sigma-Aldrich, Missouri, USA) supplemented with 2% FBS prior to nutrient challenges of 20 mM glucose and 1 mM oleic and linoleic acid for 2 h (#L9655, Sigma-Aldrich, Missouri, USA) with or without 3 nM human insulin (NNC0121-0308) and 30 nM S961 (NNC0069-0961) as indicated. The background and control human organoid treatments were DMEM low glucose supplemented with 0.1% human serum albumin (Cat. No. A1887, Sigma-Aldrich, Missouri, USA) for 2 h. Immediately after the nutrient challenge, human intestinal organoids were placed on ice and media was collected for LEAP2 ELISA. 350 μL of RLT lysis buffer (Qiagen) were added directly to the Matrigel domes with organoids while on ice, the domes with organoids were dissociated and dissolved by pipetting and scraping, and lysates were collected in Eppendorf tubes for RNA extraction and qPCR as described above.

Crypt isolation and mouse intestinal organoids

Mouse intestinal crypts were isolated from C57BL/6J mouse jejunum, as described previously[52–55] and were seeded into Matrigel (BD Biosciences), in which they grew into organoids.[53,55] Crypts were established and maintained in Complete IntestiCult Organoid Growth Medium (Mouse) (Cat. No. #06005, Stemcell Technologies, Vancouver, Canada) according to manufacturer's protocol. The

medium was refreshed every 2 days. Analysis of freshly un-passaged intestinal mouse organoids was performed on 5-7 days-old cultures, when crypts from the small intestine had budded. On the day of the experiments, mouse organoids were partially starved for 4h in Dulbecco's Modified Eagle's Medium (DMEM) – low glucose supplemented with 2% FBS, 1:1000 mouse RSPO (#3474-RS, Biotechne), 1:1000 mouse Noggin (#6997-NG, Biotechne), and 1:2000 mouse EGF (#2028-EG, Biotechne) prior to the same 2 h nutrient challenge as with the human intestinal organoids. Harvesting of organoids and collection of media were performed in the same way as with human intestinal organoids.

Cell lines

For insulin stimulation, cells were incubated with 3 nM human insulin for 18 h. For culturing in insulin resistant medium, HepG2-IGF1R-KO cells were exposed to 1 nM human insulin, 0.5 mM palmitic, linoleic, and oleic acids, and 20 mM glucose for 72 h prior to insulin stimulation. RNA for bulk RNA-seq was isolated using RNeasy Mini Kit with DNase treatment according to manufacturer's instructions (Qiagen, Hilden, Germany), and the sequencing library was prepared by purification of poly-A containing mRNAs, mRNA fragmentation, strand-specific random primed cDNA synthesis, and adapter ligation and adapter specific PCR amplification using the NEBNext Ultra II Directional RNA Library Prep Kit for Illumina (NEB #E7765, New England BioLabs, Ipswich, Massachusetts, USA). The sequencing was performed on the Illumina paired-end read sequencing (2 x 150 bp, minimum of 30 M read pairs +/− 3%) platform (Eurofins, Germany site). All RNA samples had RIN scores of 9.8–10. Bulk RNA-sequencing reads from HepG2-IGF1R-KO cells were aligned to GRCh37 using Salmon[49] and quantification was performed using STAR. Fastq files were quality-controlled using MultiQC. Differential expression analysis was performed in R using DEseq2.[50] The adjusted *p*-value cutoff was set to 0.05. The Log2Foldchange cutoff was set to 0. Appropriate normalization was evaluated by MA-plotting. Stable shrinkage procedure was evaluated by shrink-dispersion plotting. Uniform *p*-value distributions reflecting null and alternative hypotheses and a well-specified mode were evaluated by *p*-value distribution plotting.

Bioinformatics

To determine the cell type source of human LEAP2 liver gene expression, we investigated its expression across a comprehensive liver cellular atlas. We integrated six independent studies of liver cell snRNA-seq and scRNA-seq data. Count matrices from GEO accessions GSE136103, GSE185477, GSE189175, GSE189600, GSE192740, and GSE212837 were concatenated retaining the intersected genes across studies. Barcodes with extreme sequencing depth (1%) and more than 25% mitochondrial transcripts were filtered out. Liver cell types were identified by Leiden clustering a cell nearest neighbor graph where technical effects had been accounted for using the BBKNN approach.[58] Such cell graph was initially build based on cell-to-cell similarities in the top 30 principal components of the top 1000 most variable genes across all cells. Cell embedding and clustering were performed using scanpy v1.9.3.[59] Cell type identity was defined by annotating the least granular clustering resolution with the highest average silhouette score. Cell cluster-specific genes were identified using the Mann-Whitney-Wilcoxon test and contrasted with well-known cell-type-specific genes to define the cluster cell identity.

In the UCSC Genome Browser (GRCh38/hg38), we used the ensemble gene ID ENSG000000164406.7 (RefSeq NM_052971) on genomic position hg38 chr5:132872322-132875046 to examine human LEAP2 gene expression from the NIH Genotype-Tissue Expression (GTEx) project (release V8) track. This track is based on data from 17,382 tissue samples obtained from 948 adults post-mortem. Statistical analysis and data interpretation was performed by The GTEx Consortium Analysis Working Group.[60–62] Data was provided by the GTEx LDACC at The Broad Institute of MIT and Harvard. In the GTEx portal, we extracted data from bulk tissue gene expression for human LEAP2 (data source: GTEx Analysis Release V8 dbGaP Accession phs000424.v8.p2). For bulk tissue RNAseq, expression values are calculated as transcripts per million (TPM) from a gene model with isoforms collapsed to a single LEAP2 gene. Boxplots are shown as medians with 25th and 75th percentiles. All ChIP data, ATAC-seq, bisulfite-seq, and DNase-seq data are from the ChIP-Atlas[63,64] and were filtered for either liver data, digestive tract data or hepatocyte data, and visualized in the Integrative Genomics Viewer (IGV) software. We used the hg38 assembly for human data and the mm10 mouse assembly for mouse data, and data were mapped to chr5:132,868,190-132,884,003 and chr11:53,415,595-53,428,959, respectively. All transcription factor binding data were mapped to this region. Subsequently, transcription factors found to be regulated by insulin and glucagon were filtered for manually in the ChIP-Atlas. Conservation data was acquired from the UCSC genome browser track Vertebrate Multiz Alignment & Conservation (100 Species), which are available as PhyloP conservation (WIG format) and was visualized in IGV. Data from ENCODE Candidate Cis-Regulatory Elements (cCREs) were downloaded from the UCSC browser download server as a BigBed file and visualized in IGV. Bulk RNAseq data from the Gene Expression Omnibus (GEO) were acquired from the GSE110673[65] and the RPKM matrix was gunzipped locally.

QUANTIFICATION AND STATISTICAL ANALYSIS

Statistics were performed using R statistical software (R Core Team (2023). R: A language and environment for statistical computing. R Foundation for Statistical Computing, Vienna, Austria. URL https://www.R-project.org/R version 4.2.3 (2023-03-15 ucrt)) and GraphPad Prism 10 (GraphPad). For parametric data, differences in means across groups were tested by Welch's t-test or one-way ANOVA. For nonparametric data, Mann-Whitney or Kruskal Wallis tests were used to test differences in medians between two or more groups, respectively. Inspection of Q-Q plots in R was used to assess Gaussian distribution of collected data. Statistical

significance was defined by a *p*-value less than 0.05, and data are shown as bar graphs with individual data points unless otherwise stated. Continuous data were checked for any violations of the assumptions necessary to run one-way ANOVAs with repeated measures. Repeated measures correlations were calculated using the rmcorr package. If the *p*-value was significant, appropriate post-hoc multiple comparisons tests were performed, as indicated. Correction for multiple testing as indicated. DEseq2 uses generalized linear models and Wald tests to test for differential expression. Statistical details of statistical test used, sample size, what the sample size represents, and definition of center and precision measures can be found in the figure legends or the "method details" for each of the experiments.

ADDITIONAL RESOURCES

Clinical trial registries and links

Clinical trial NCT04859322 on clinicaltrials.gov: https://clinicaltrials.gov/study/NCT04859322.

Clinical trial NCT02475421 on clinicaltrials.gov: https://clinicaltrials.gov/study/NCT02475421.